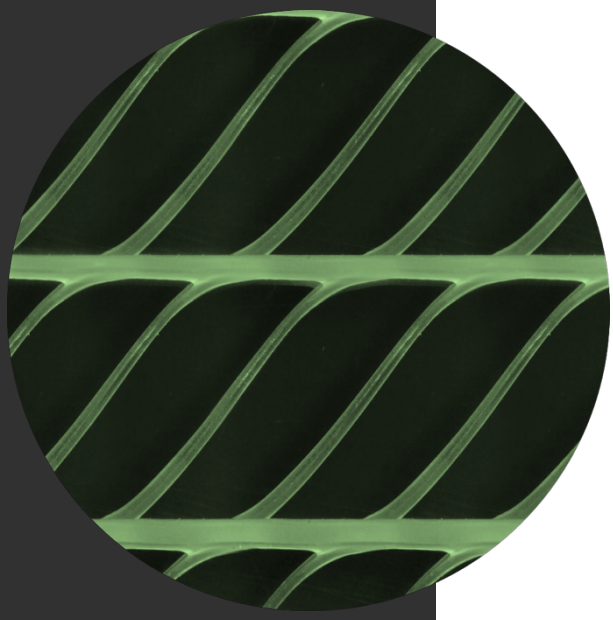

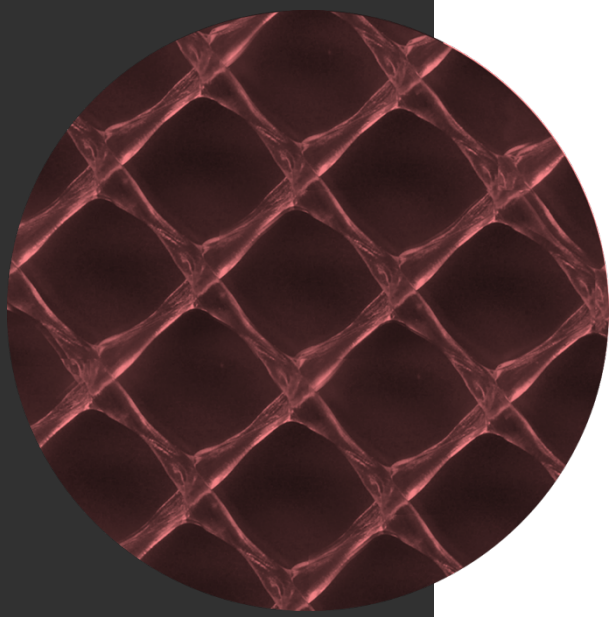

# Master thesis

## Crossflow reversal effect on removal of RO particulate fouling: a comparison of two spacers

Felipe González

TU Delft Delft University of Technology

# Crossflow reversal effect on removal of RO particulate fouling: a comparison of two spacers

Felipe de Jesús González González

For the degree of Master of Science in Civil Engineering, specialized in Sanitary Engineering

---

Assessment committee:

Prof. Dr. Ir. Jules van Lier, section of Sanitary Engineering, Delft University of Technology
Dr. Ir. Henri Spanjers, section of Sanitary Engineering, Delft University of Technology
Dr. Ir. Santiago Pacheco-Ruiz, Biothane Veolia Water Technologies
Dr. Ir. Amir Haidari, section of Sanitary Engineering, Delft University of Technology

External committee member:

Prof. Dr. Geert-Jan Witkamp, Applied Sciences Faculty, Delft University of Technology

Section of Sanitary Engineering, department of Watermanagement
Faculty of Civil Engineering and Geosciences
Delft University of Technology, Delft, The Netherlands
Submitted on 3 October 2017

TU Delft Delft University of Technology

BIOTHANE Leading Anaerobic Technologies

# ABSTRACT

Worldwide fresh water scarcity is nowadays becoming a reality rather than a futuristic concern. Non-conventional sources of wastewater are being considered as a solution for this problem, since fresh water sources will not be sufficient to satisfy the world's water demand in the following years. Extensive research is being done on different wastewater treatment technologies and methodologies, and lately, reverse osmosis (RO) membrane filtration has caught more attention as a solution for reclaiming and reusing wastewater. Nevertheless, the biggest problem RO membranes face is fouling, which increases energy consumption, and therefore, costs. Organic/particulate fouling affects the mass transfer of an RO membrane, but it can also contribute to biofouling, worsening the mass transfer and causing pressure drop on the RO system.

For this study, a RO crossflow cell was used in order to investigate the effect of crossflow reversal on particulate fouling removal by testing two different feed spacers: (a) 1.25-mm high cavity spacer and (b) 0.71-mm high zigzag spacer. The experiments were carried out with an average crossflow velocity of 0.36 m/s, an average permeate flux of 20 L/m$^2$·hr (LMH), an average feed electroconductivity (EC) of 14.90 mS/cm, and a feed temperature in the range of 21-25 °C. Four runs were done, each with an average runtime of 1050 minutes. Two runs tested the cavity spacer, one with a crossflow reversal done at minute 806, and the other run with a crossflow reversal done twice every working day. The last two runs follow the same methodology but using the zigzag spacer. Each run used a new membrane and spacer. The mass transfer was graphed as a Mass Transfer Coefficient (MTC), and its development with time was analysed for identifying fouling, as well as particulate fouling when applying the crossflow reversal method.

Crossflow reversal proved to be a reliable method for removing organic/particulate fouling. The cavity spacer caused a more severe organic/particulate fouling, but allowed it to be removed by crossflow reversal. The cavity spacer also proved to be less energy-consuming if applied to a full-scale RO facility. On the other hand, the zigzag showed to have a better effect on flow mixing and concentration polarization disruption inside the feed channel, thus keeping a higher mass transfer for a longer period of time. A more frequent crossflow reversal showed was not more efficient in removing organic/particulate fouling.

# ACKNOWLEDGEMENTS

As my family, friends, and life itself have well taught me to be grateful towards the others, in the next set of words I would deeply like to express how grateful I am towards everyone who was involved in the realization of this Master thesis.

First of all, I want to thank my parents, who raised me with all love and inculcated in me the habit of loving life as much as they love me; who taught me how to find my purpose in this world. I want to thank my father, who showed me that the concept of "work" doesn't exist whenever you love what you do for a living, and that serving the others with honesty is a key value in one's career. I want to thank my mother, who has always been there for me in my most difficult moments through life; who has showed me how to stand up when fallen; who has made me understand that the limits in this life are inside oneself. I want to thank my brother and my sister, for believing in me and for motivating me, making me realise that all my effort in what I do is a great example for them.

I also want to thank all the rest of my family, my friends, and my girlfriend, who were always close to me even though I'm far away from them; who supported me with whenever I felt lonely and disoriented; who believed in me all the time. I want to specially thank my girlfriend, who unconditionally supported me in the last stage of my MSc thesis; who made me realise I was capable of fulfilling this thesis, and more; who always had and has confidence on me.

I want to thank the National Council of Science and Technology in Mexico (CONACYT) and the Council of Science and Technology of San Luis Potosí (COPOCYT) for making my MSc studies possible; their values, vision and financial support gave me the opportunity to fulfil one of my biggest ambitions of this stage of my life. I want to thank Biothane-Veolia for allowing me to do this project with them, trusting in me, and always pushing me a bit further. I want to thank TU Delft and its staff, my teachers and professors, and all my classmates who enriched this MSc experience and made it possible; each one of the persons I met at TU Delft contributed to my journey.

Last but not least, I want to thank my evaluation committee for supporting me, for guiding me, and for trusting in my independency and capability of fulfilling this MSc degree. They were a clear example of academic and professional success, they were always a motivation to me, and they contributed to my professional growth, transforming me in a person with more capability and bigger ambitions.

## Important for the reader

This MSc thesis project was done in collaboration with Biothane – Veolia.

For the following document, it is important to make clear to the reader that the Master thesis project showed in this document will be referred to as "**the Project**"; the company that provided the case and materials for coming up with **the Project** will be referred to as "**Biothane**"; and last but not least, Delft University of Technology, will be referred to as "**the University**".

The front page of this study was designed by Arch. Juan Jose Dibildox Gonzalez.

# ACRONYMS

| | |
|---|---|
| AnMBR | Anaerobic Membrane Bioreactor |
| CIP | Cleaning in place |
| COD | Chemical oxygen demand |
| CTA | Crude terephthalic acid |
| DMT | Dimethyl terephthalate |
| DO | Dissolved oxygen |
| EC | Electroconductivity |
| LMH | Liters per square meter per hour |
| MF | Microfiltration |
| MLSS | Mixed liquor suspended solids |
| MTC | Mass Transfer Coefficient |
| NDP | Net driving pressure |
| ORP | Oxidation reduction potential |
| PLC | Programmable logic controller |
| PTA | Purified terephthalic acid |
| RO | Reverse osmosis |
| TCF | Temperature correction factor |
| TKN | Total Kjeldahl Nitrogen |
| TMP | Transmembrane pressure |
| UF | Ultrafiltration |
| VFA | Volatile fatty acids |

# TABLE OF CONTENTS

# 1. INTRODUCTION

Water is life, humans cannot live without water, and imagining this world without water it's impossible. Water has been used by humanity for its entire existence for many different activities. Wastewater is a by-product of these activities, and up to today wastewaters are not well managed globally.

Approximately 80% of the world wastewaters are not treated, and are later discharged to the environment, polluting many ecosystems, such as the marine ecosystem, which by now reaches a polluted area of seas and oceans that add up to more than 245,000 $km^2$ (UN Water, 2017), similar to having a huge polluted lake the size of the United Kingdom. This means that the aquatic flora and fauna that we consume are contaminated, and therefore, we are indirectly affected by this pollution through the food chain in this ecosystem. Untreated wastewaters also cause severe pollution to many of our fresh water sources, such as rivers and aquifers, and consequently cause waterborne diseases and even death when these waters are used and/or consumed. United Nations (United Nations, 2016) reported that close to 1.8 billion people around the world have access to drinking water sources that are faecally polluted, and that around 1.7 billion people live in river basins where the water resources are over-exploited, in other words, the extraction and use of water resources goes beyond the recharge capacity. As population increases worldwide, the demand for freshwater sources is growing alarmingly due to the varying water consumption patterns, as well as climate changes (Haidari et al., 2017), and as a consequence, different water sources have been lately being used for human use and consumption.

We are facing many other problems nowadays regarding the use and quality of water, however, this thesis project cannot focus on all the global water issues, therefore, it's important to define and specify the problem even more, and industrial wastewater is the topic of study. Industrial wastewater is basically the water that has been used, polluted and discharged in any industrial cluster, such as chemical, petrochemical, food and beverages, pharmaceutical, textile, mining, etc., just to mention a few examples.

The world water withdrawal per sector by 2010 was estimated to be 69%, 19% and 12% for agricultural, industrial and municipal use, respectively. For Europe alone, the fractions withdrawn were 21%, 57% and 22% for agricultural, industrial and municipal use, respectively

(AQUASTAT, 2016). Industrial processes can heavily pollute water sources and can consume very high amounts of water, thus, the urge to treat and recycle the industrial wastewaters in order to secure the water quality and availability.

There are several water treatment technologies and combinations of them that can be used in order to treat wastewater up to the point of reuse, and Reverse Osmosis (RO) membrane filtration is one of them. RO membranes is a very promising water treatment technology that initially started to be used for obtaining pure water from seawater or brackish water (DOW, 2013), but just recently it has become more attractive due to the lack of freshwater sources and the need of reclaiming and reusing wastewater (Into et al., 2004). Nowadays many industries, such as food and beverage, pharmaceutical (Goosen et al., 2005), mine and cooling water (Buhrmann et al., 1999), chemical, textile, pulp and paper, petrochemical, tanning, metal finishing (Bódalo-Santoyo et al., 2003), dairy (Vourch et al., 2008), among some others, rely on this technology for reclamation of their wastewaters with a relatively decent energy consumption (Bódalo-Santoyo et al., 2003), thanks to the ability for removing on average more than 95% of all dissolved salts, inorganic and organic molecules of a molecular weight of approximately 100 g/mol and higher, depending on the design and operation of the membrane installation, as well as the wastewater characteristics (DOW, 2013). It is implicit in the molecular weight rejection of RO membranes that any type of pathogen is removed with a 100% efficiency, nevertheless, this subtopic is not part of **the Project** and won't be discussed.

One of the major disadvantages in using RO membranes is the increase in the energy required to operate them, since the membranes begin to foul and the pumps need to increase the feed pressure in order to produce the same permeate flow.

Fouling on RO systems can be attributed to (i) biofilm growth on the feed spacers (Vrouwenvelder et al., 2009), (ii) organics and particulates that aggregate, chelate and deposit on the areas with a low crossflow velocity along the feed spacers (Haidari et al., 2016), and (iii) dissolved ions that crystallize on the membrane's surface (Goosen et al., 2005). The former phenomenon is called scaling.

RO systems tend to have scaling problems due to minerals that precipitate on the membrane. This mineral precipitation occurs when exceeding the mineral concentrations over the solubility limits of these minerals when the permeate recovery rate increases. Scaling causes a reduction in permeate production which needs to be compensated by increasing the applied pressure and thus, the operational costs of the system.

Additionally, organic and particulate fouling, which are related to biofouling due to the deposited substrate that is available for bacterial growth, are a problem attributed to poor flow mixing caused by the mere geometrical configuration of the feed spacers (Bucs et al., 2013; Radu et al., 2014; Vrouwenvelder et al., 2009). Consequently, biofouling increases the pressure losses, thus, coming back to the main problem: increased energy consumption in the RO system.

Pressure losses parallel to a decreased permeability are problems directly attributed to fouling, and fouling is a problem attributed to feed spacers. However, fouling has caused research projects to focus on membrane development for many years, but very rarely towards the development of feed channel spacers. By 2009, barely any research on feed spacers could be tracked on databases or other kinds of media, like conferences (Vrouwenvelder, 2009; Vrouwenvelder et al., 2009). As a consequence, new studies on feed spacer adaptation have emerged, together with new methodologies for cleaning/removing fouling occurring in the feed channels of RO membranes.

The mere presence of feed spacers in the feed channels is not the responsible for fouling, but a set of geometrical features of the spacers. These features, such as spacer height, angle between the filaments that constitute the spacer, diameter of the filaments and separation between them, among others, have been found throughout research to have an effect on the feed channel's flow turbulence, disruption of the concentration polarization layer, variations of velocity throughout time and space in the feed channel, shear forces on the membrane, changes in flow direction along the spacer, and energy losses expressed as pressure drop (Bucs et al., 2013; Da Costa et al., 1994; Haidari, 2017; Haidari et al., 2016; Koo et al., 2015; Subramani & Hoek, 2008; Zimmerer & Kottke, 1996).

By studying and improving the aforementioned spacer features and their effect on different parameters inside the feed channel, fouling can be fought. Nevertheless, modifying the spacer might not be the only solution to the problem. Already other studies have proposed to apply physical measures to remove and control fouling, such as reversing the direction of the flow inside the feed channel (Belfort et al., 1994; Vrouwenvelder et al., 2011). Crystallized minerals (scaling) on the membrane might be difficult to remove by crossflow reversal because of the strong and rigid structure they form (Mullin, 2001), while biofouling has been reported to be hard to remove when it becomes "thin and compact" with a higher shear stress (Vrouwenvelder et al., 2011). However, if the deposited particles that can serve as substrate for bacterial growth are removed by crossflow reversal, biofouling could be controlled at some extent (Subramani & Hoek, 2008; Vrouwenvelder et al., 2011), not to mention that

organic/particulate fouling itself would be removed. Therefore, the attention now turns to organic/particulate fouling removal.

Diversity in the composition of different wastewaters and the urge to reuse them is causing the beginning of a new era in RO treatment: fouling matters will gain complexity, and research on RO membranes and feed spacers will grow. Nevertheless, studying the effect of crossflow reversal on organic/particulate fouling is already a good start.

## 1.1 General description of the Project

### 1.1.1 The actual situation

At **Biothane**, the core wastewater treatment technology is anaerobic digestion. For **the Project**, an RO system is used, preceded by an Anaerobic Membrane Bioreactor (AnMBR), a water treatment technology that combines filtration membranes and anaerobic digestion. The AnMBR is a lab-scale equipment located at the facilities of **Biothane.** The petrochemical wastewater treated by the AnMBR comes from the production of Purified Terephthalic Acid (PTA), which is the raw resource in the production of polyesters. The PTA wastewater is synthetized at **Biothane**'s laboratory. The pollutants in the wastewater, which represent a relatively high concentration of chemical oxygen demand (11 g COD/L), are not completely removed by the AnMBR and are still a threat to the environment. Therefore, a post-treatment step has been proposed by **Biothane** in order to be able to not only discharge the treated water to the environment, but to actually reuse it. This post-treatment consists of RO membrane filtration, which is fed with the permeate of the AnMBR.

Having given the opportunity to work with RO technology at a lab-scale, optimization of this part of the treatment train (AnMBR-RO) could be analysed, being RO-fouling the problem of interest.

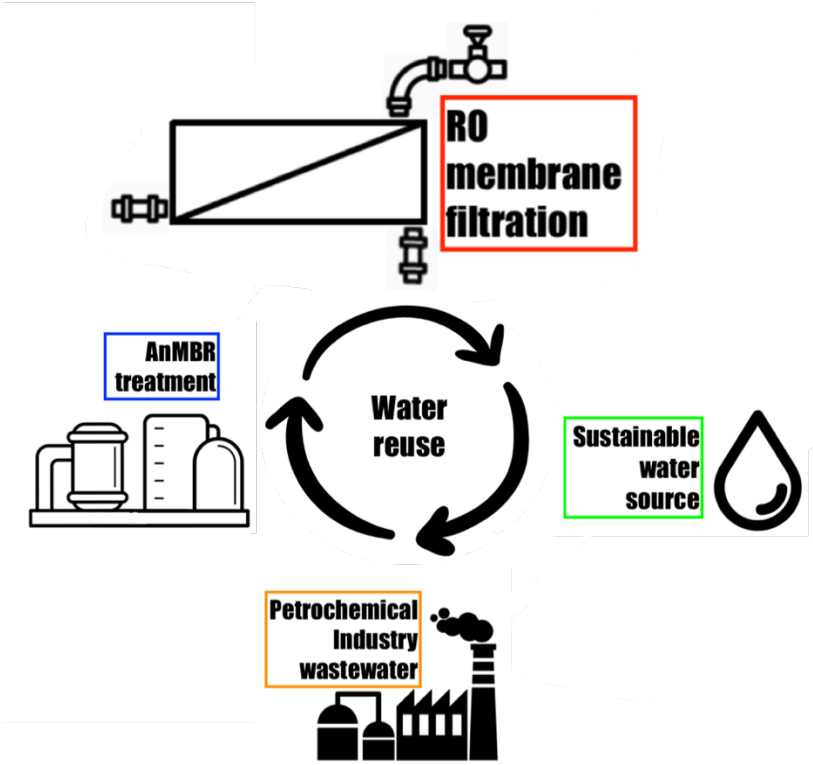


**Figure 1: Biothane's current proposal for water reuse. RO membrane filtration as the improvement step. The final effluent results in a sustainable water source for different purposes.**

### 1.1.2 The Project's problem of interest

RO membranes can be highly energy-consuming because of the high pressures needed to produce clean water, and this energy consumption always increases with time due to fouling. The former phenomenon reduces the permeate flux (flow per unit area), resulting in an increment of pressure needed for producing the desired permeate flux, as many RO facilities operate under a constant permeate flow, and not a constant feed pressure.

Current methods for controlling/removing fouling are chemical cleaning of the RO membranes and the use of low-fouling membranes, which are not always the best solution (Vrouwenvelder et al., 2011). Fouling, therefore, is one of the biggest disadvantages of RO membrane filtration, and this has recently made researchers to study the effect of feed spacers on fouling.

### 1.1.3 The solution proposed for the Project:

Extensive research has been done on the development of reverse osmosis sheet membranes, but not a lot on the feed spacers (Vrouwenvelder, 2009; Vrouwenvelder et al., 2009); moreover,

it has already been reported that reversing the direction of the feed flow may contribute to particulate re-suspension from the membrane, consequently controlling fouling (Belfort et al., 1994; Vrouwenvelder et al., 2011). Therefore, the use of a different type of feed spacer (Figure 2) than the common feed spacers used in RO, together with crossflow reversal, as shown on Figure 4, have been proposed as a solution for efficiently removing/controlling the fouling occurring on the RO membrane. The conventional zigzag spacer (Figure 3) is also tested with the crossflow reversal methodology. Using a different feed spacer in an RO facility could not only mean an improvement in the permeate flux, but also in the pressure drop, saving energy and making RO treatment technology even a more attractive solution towards wastewater reclamation and reuse.

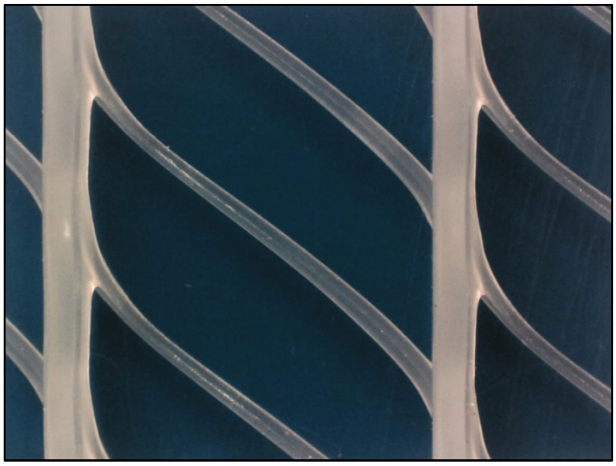

**Figure 2: newly proposed cavity spacer, flow goes from the superior part of the picture to the inferior part. Image obtained from** (Haidari, 2017).

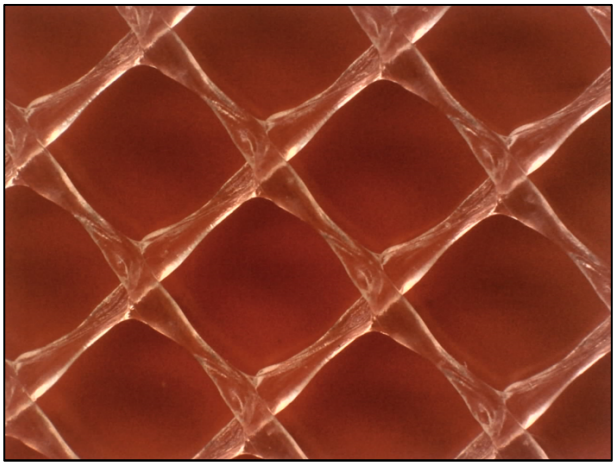

**Figure 3: conventional zigzag spacer, flow goes from the superior part of the picture to the inferior part. Image obtained from** (Haidari, 2017).

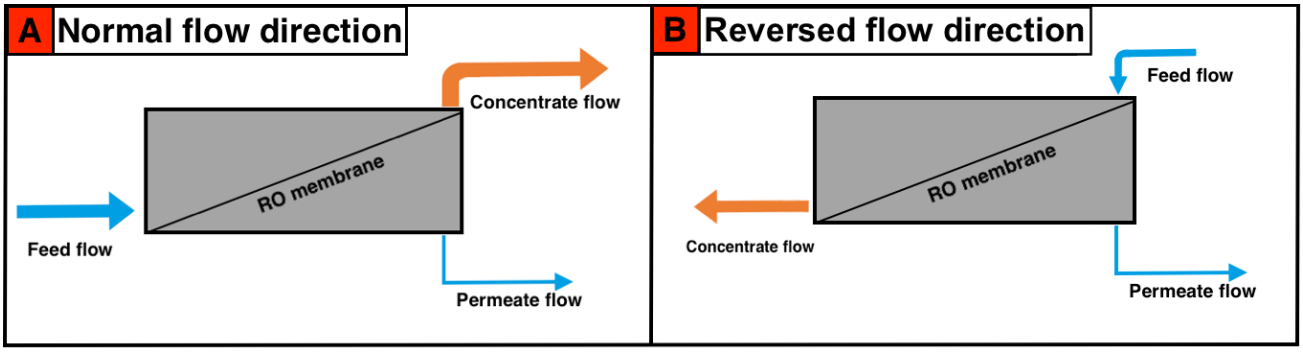


**Figure 4: Representative scheme of the standard operation of an RO membrane element (A), and the proposed solution for fouling removal, where the flow direction is reversed (B), entering from the concentrate side, and exiting from the feed side.**

### 1.1.4 Objective

The goal of **the Project** is expressed in the next research questions:

1. Which feed spacer, (a) conventional 0.71-mm high zigzag spacer or (b) 1.25-mm high cavity spacer, is the most efficient at organic/particulate fouling removal/control expressed as a Mass Transfer Coefficient (MTC) development, by the effect of the crossflow reversal method in the feed channel: supplying the water to be treated from the concentrate side instead of supplying from the feed side of the RO membrane?
2. Which feed spacer, (a) or (b), is a better option at delaying organic/particle fouling when no crossflow reversal is applied?
3. Which feed spacer is more energy-efficient in terms of pressure drop if applied to a full-scale reverse osmosis facility?

## 1.2 Approach

Once the objective of **the Project** has been defined, a methodology is structured, accompanied by the corresponding theoretical background that supports it. The next chapters give structure to the thesis, beginning with the theory involved in **the Project**, followed by the materials and methodology used in order to achieve the objective of **the Project**. The previous sections allow to interpret the results, which are shown together with their corresponding discussion. Finally, the conclusions are summarized in a separate section, and based on this, the final recommendations are presented.

**Biothane's** solution to an improved AnMBR effluent consists, as previously explained, of a RO post-treatment. First, an introduction to the lab-scale AnMBR is done (section 2.1), so that it is clear how the feed to the RO system was obtained. Secondly, it is important to understand the general composition, configuration and operation of RO membrane technology (section 2.2). Fouling is then addressed (section 2.2.1) as one of the main problems that RO membranes face, and a deeper explanation of how this phenomenon relates to specific factors of RO membranes, is done. One of the previously mentioned factors is the feed spacers, which are the main focus of the study. The theory behind feed spacers is presented (section 2.3), allowing to understand how fouling is dependant of the type of spacer used. A non-intrusive method to measure fouling is the use of a coefficient called Mass Transfer Coefficient (MTC) (section 2.4). The MTC

is a numerical tool that expresses the volume of water passing through a unit of membrane when a unit of available driving pressure is applied to the membrane.

The materials (section 3.1-3.3) and methodology (section 3.4-3.5) used in this study are supported by the theory explained in the previous paragraph. First, the materials required for carrying out the experiments are described, and secondly, the methodology of the experiments is explained in detail.

Last but not least, the results are shown and discussed (chapter 4), and posteriorly summarized on conclusive points of view (chapter 5) with final recommendations for future stages of **the Project's** field of research and implementation in full-scale RO facilities.

# 2. THEORY BEHIND THE PROJECT

## 2.1 Anaerobic Membrane Bioreactors

Anaerobic wastewater treatment, a biochemical process in which the organic matter is degraded and mostly methane and carbon dioxide are produced, compared to conventional activated sludge treatment has proven to be a robust technology that can handle higher substrate loads. In other words, higher concentrations of chemical oxygen demand (COD) per unit of volume can be biologically treated by anaerobic wastewater treatment. Additionally, this treatment has several other advantages, such as a smaller footprint, less energy consumption due to the unnecessary reactor aeration, approximately 90% less sludge production, and it can generate energy via methane production (van Lier et al., 2008).

As a complement to the advantages of the anaerobic treatment, using membranes to increase the concentration of Mixed Liquor Suspended Solids (MLSS), allowing smaller reactor volumes with a smaller footprint (Lousada-Ferreira, 2011b), results in an outstanding combination of these two water treatment technologies. This combination is called Anaerobic Membrane Bioreactor (AnMBR), and produces an effluent of high quality and highly disinfected (Metcalf & Eddy, 2003). In theory, any combination of a membrane separation process with a biological wastewater treatment is called Membrane Bioreactor (MBR) (Judd, 2011b).

The type of membranes used in MBRs/AnMBRs are usually microfiltration/ultrafiltration (MF/UF) membranes, with a nominal pore size within the range of 0.05-1 μm and 0.002-0.05 μm respectively, however, nanofiltration membranes are also a possibility. MF/UF membranes prevent suspended matter (e.g. biomass, colloids, viruses, etc.) from passing through the membrane pores, but at the same time allow dissolved solids, thus, preventing an increase in salinity inside the reactors (Judd, 2011a). Nanofiltration membranes on the other hand, are able to reject polyvalent ions (e.g. calcium), consequently increasing the concentration of salts in the bioreactor. High salinity in MBRs/AnMBRs is not desired, because it can cause problems in the physicochemical, microbiological and membrane performance (Lay et al., 2010). However, it's not in the scope of this study to discuss the problems that increased salinity can cause in MBR's, but in RO systems.

The two common configurations of AnMBR's are (i) sidestream and (ii) immersed, shown on Figure 5. The configuration used at **Biothane** is sidestream.

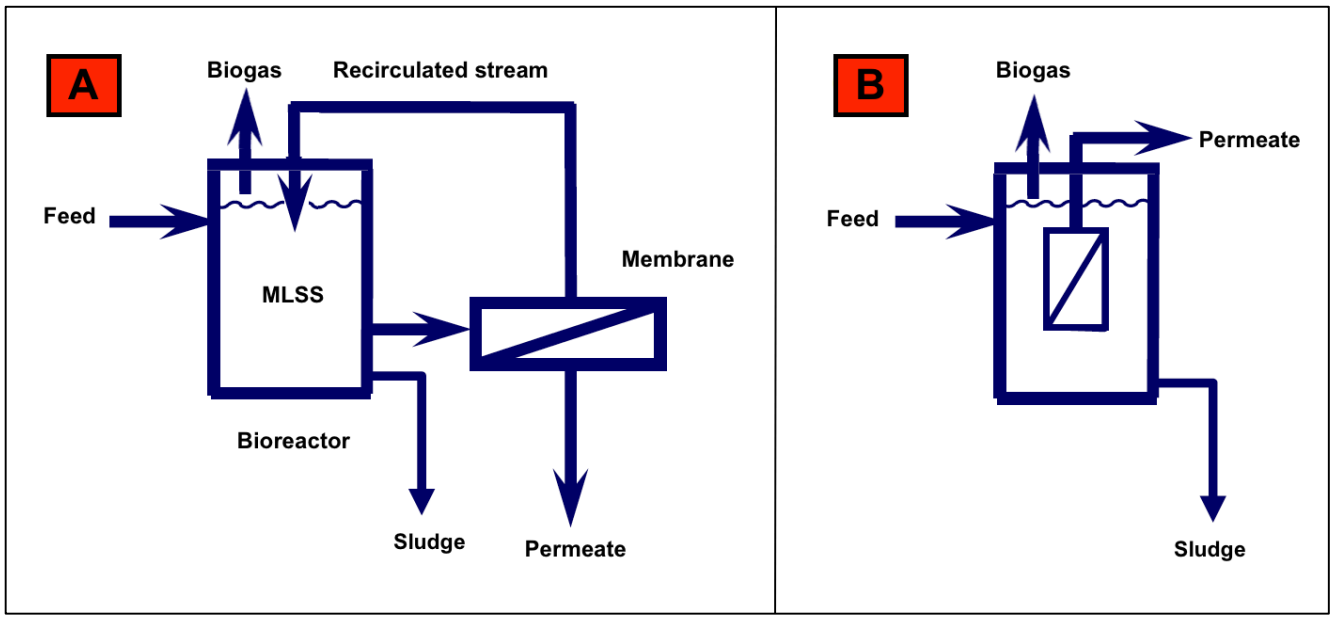


**Figure 5: Common two configurations for AnMBR's. The sidestream configuration (A) pumps the MLSS out of the reactor, along the membrane, and circulates it back to the bioreactor. In the immersed configuration (B), the permeate is sucked out of the bioreactor. This last configuration doesn't have a recirculation line, since it has the membranes immersed in the MLSS. Image modified from** (Judd, 2011b).

Normally, UF is applied as a pre-treatment prior to RO membranes (Goosen et al., 2005). It is then presumed that AnMBR/UF can lead to an improved performance of the RO post-treatment, thanks to (i) a decreased RO-biofouling potential due to lower biological activity attributed to the anaerobic conditions, and to (ii) a very low concentration of particles and colloids attributed to the UF rejection capacity.

## 2.2 Reverse Osmosis Membranes

Reverse Osmosis membrane filtration is not a new water treatment technology, it has already been in use for sea water and brackish water desalination since the early 1960's, however, its application has become more diverse since freshwater sources have started to be depleted and new unconventional water sources began to be seen as a solution to the water scarcity (DOW, 2013).

RO membrane technology is a semi-permeable layer that allows water through it but retains almost all dissolved matter when a certain pressure is applied according to the ion concentration present in the water that wants to be filtered through the membrane (Fritzmann et al., 2007), this means, the higher the concentration of ions in the water to be filtered, the more pressure needed in order to make the water molecules go through the membrane. In other

words, RO membrane filtration is a pressure-driven technology that can achieve the highest removal efficiency of pollutants in the water. Nevertheless, pressure is not the only factor to consider for obtaining a pure permeate effluent with RO membranes, there are some other factors and elements that have made researchers look into this membrane technology for many years and have gradually let engineers understand in more detail how RO membrane filtration works, what are the limitations, improvements, new application fields, etc.

Reverse osmosis is literally the inversed phenomenon of osmosis. Osmosis happens when pure water goes through a semi-permeable membrane from a less concentrated solution of salts to a more concentrated solution, this in order to dilute the concentrated solution and to keep both solutions on the same concentration. If osmosis were to happen in a container with a semi-permeable membrane in between, and two initial solutions with different ion concentrations on each side of the membrane, the water column gained on the diluted side of the membrane would equal to the osmotic pressure that the concentrated side of the membrane had initially. If this water column gained wants to be filtered back to the other side of the membrane, then this action is denominated as "reverse osmosis", as shown on Figure 6 .

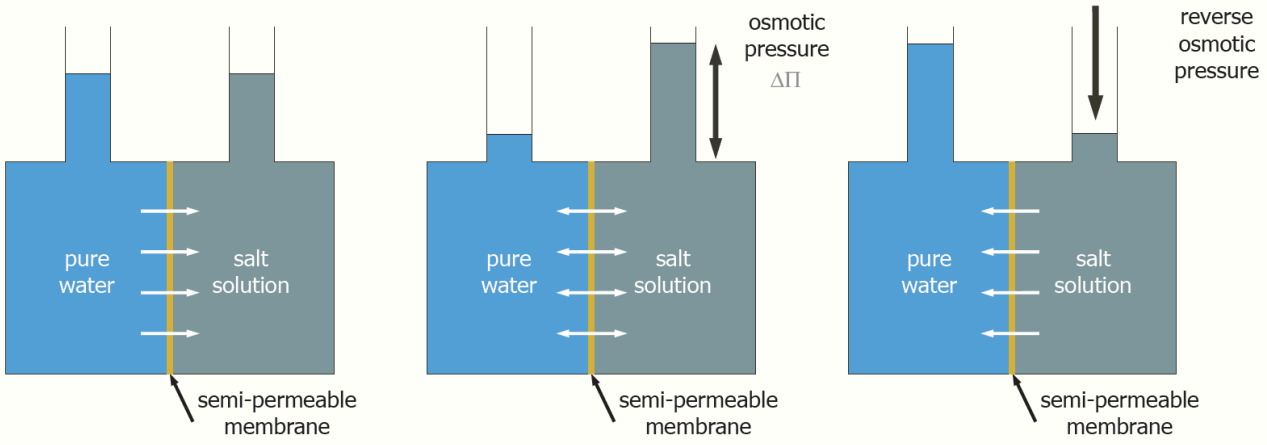


**Figure 6: Osmosis phenomenon and the osmotic pressure expressed as a water column. Image obtained from** (van Halem et al., 2009b).

The standard configuration of a RO membrane is spiral-wound. This configuration is not only used for RO membranes but also nano-filtration membranes, since it is cheaper to have more filtration area in less volume occupied by the membrane element. Spiral-wound configuration is assembled by three main components as shown in Figure 7.

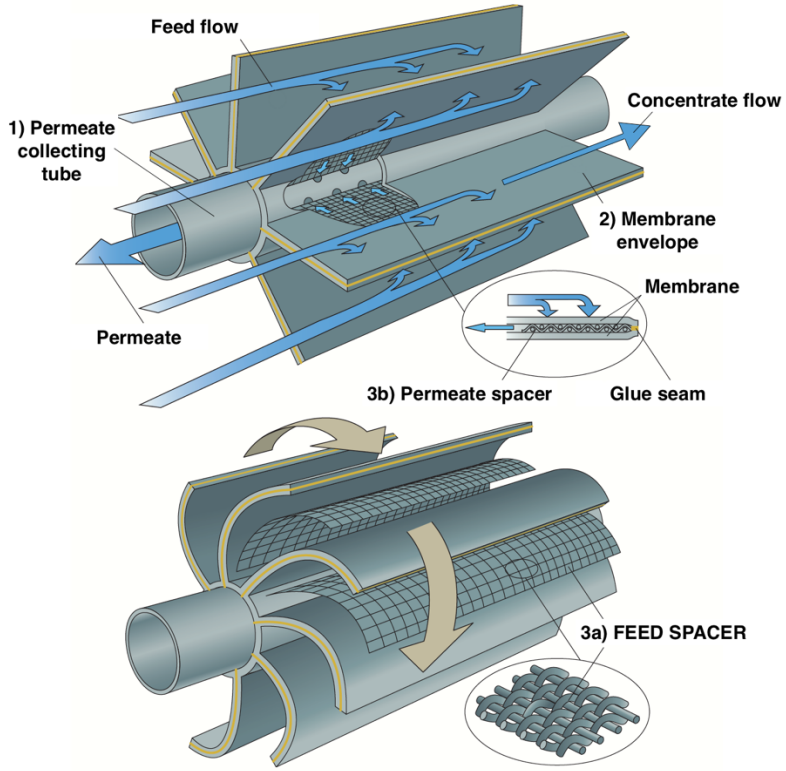


**Figure 7: An RO element configured as spiral wound. The RO element has three main components, (1) the permeate collecting tube, (2) the membrane envelopes, (3a) the feed spacers that separate the envelopes from each other and (3b) the permeate spacers that are inside each envelope in order to separate the membranes from each other. Image modified from** (van Halem et al., 2009b)**.**

Figure 7 shows the direction of the flow inside the RO membrane. Water flows from one end of the membrane element to the other end (from the "feed side" to the "concentrate side"), and permeation occurs in the same direction. This flow happens inside a pressure vessel that can contain up to eight RO elements (Metcalf & Eddy, 2003), as shown on Figure 8. The way that spiral wound membranes operate is called crossflow, where there is one stream entering, the feed stream, and two streams exiting, (i) the concentrate stream and (ii) the permeate stream.

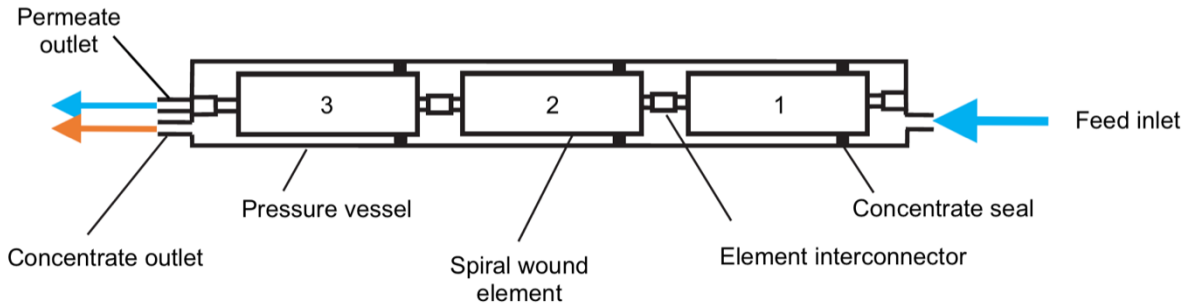


**Figure 8: RO pressure vessel. The water is input through the feed side on the right side of the drawing, goes through the first element, follows to the second element, and finally the third element on the left side of the image, where the pressure vessel finishes and the concentrate flow. Permeate produced on each element is gathered by their own permeate collecting tube, which are interconnected. Image modified from** (Metcalf & Eddy, 2003)**.**

As the water being treated flows towards the end of an element, pressure losses happen due to the hydraulic resistance induced by the feed spacer. This means that the highest pressure in an RO element is available at its beginning, and the lowest pressure at its end. The higher the pressure in the system, the higher the permeate flux (flow per unit of area), thus, obtaining a better permeate quality in terms of dissolved salts, assuming that the concentration of salts in the feed is constant.

The salt passage is independent of the pressure applied, but it's proportional to the salt difference across the membrane. Having a higher permeate flow means that the salt passing the membrane will dilute more on the permeate side of the membrane (Hydranautics, 2001). An increase in the salt concentration in the feed is translated as an increase in the salt passage, and if the permeate flux remains constant, the salts passing to the permeate will not dilute as much.

### 2.2.1 Fouling

Due to the high rejection of matter that the RO membranes have, the mass of dissolved matter is remaining almost constant inside the feed channels of the RO elements. However, the volume of water acting as the solvent is being reduced gradually as permeation occurs along the RO elements. In other words, the concentration of matter is gradually increasing as the water travels along the feed channels. This increase in concentration, particularly in salts, can trespass the solubility limit of certain ionic species present in the feed, causing mineral precipitation, which is known as scaling. The former phenomenon reduces the available permeation area of the affected membrane, consequently increasing the applied feed pressure in order to maintain the same permeate flux.

Besides scaling, another important type of fouling on RO membranes is biofouling. This type of fouling is defined as biological growth on the feed channel, which causes the pressure drop to increase (Bucs et al., 2014). This aforementioned increase can be so high that the further RO elements in the pressure vessel have a much lower net driving pressure, causing the permeate quality and quantity to worsen (Bucs et al., 2013). In order to avoid the permeate quality from worsening due to biofouling, the feed pressure applied needs to increase, resulting in a higher energy consumption for the operation of the RO system. Some studies have shown that biofouling can be controlled by reducing the concentration of nutrients in the feed, specially orthophosphates, as well as modifying the feed spacer's geometry and lowering the feed channel's crossflow velocity (Bucs et al., 2014; Vrouwenvelder et al., 2009). Biofouling has also been attributed to substrate that has been deposited on the membranes surface and has become

available for bacteria (Subramani & Hoek, 2008; Vrouwenvelder et al., 2011). This latter matter deposition is also called organic/particulate fouling.

Organic/particulate fouling might be attributed to the deposition of colloidal aggregates that form due to pH changes in the water that destabilize these particles. The colloidal aggregates can also vary in composition. Humic acids, proteins and other organic molecules can form complexes or chelates that can deposit on the membrane's surface and also on top of already existing crystal structures and scaling layers (Goosen et al., 2005). From this definition, organic/particulate fouling can be generally qualified as any type of fouling that is not bacterial growth (biofouling) nor mineral crystallization (scaling).

Energy increase in RO membranes is one of the main problems this technology is facing. Different studies are researching on ways to decrease/prevent fouling on RO membranes, as well as improving their performance: from low-fouling sheet membranes, to novel feed spacer configurations.

## 2.3 Feed Spacers

Feed spacers are essential in spiral wound membrane configurations. Feed spacers have two main functions: (1) separating the membrane envelopes in order to give structure to the feed channel, and (2) creating a hydraulic turbulence that improves the mass transfer by disturbing the concentration polarization layer that forms on the membrane (Haidari et al., 2016), in other words, improving the permeate flux.

The concentration polarization happens when water starts being permeated across the RO membrane and the dissolved salts in the feed start accumulating on the membrane surface due to the pressure difference over the membrane. If the net driving pressure (NDP) is equal to zero, then there would be no driving force for the feed to be permeated, and therefore, no concentration polarization. The higher the concentration of dissolved salts in the feed, the higher the osmotic pressure in the feed and the stronger the effect of the concentration polarization.

As already mentioned in section 2.3 and 1.1, fouling is a big issue in spiral wound membranes. Studies have proved that biofouling is problem directly attributed to the feed spacer itself (Vrouwenvelder et al., 2009). Biofouling has been reported to create such a high pressure drop due to its extreme hydraulic resistance, that feed spacers have been pushed out of place inside the feed channels (Schneider et al., 2005). Feed spacers are also known to be responsible for

problems regarding a poor flow mixing, lower mass transfer and mineral scaling (Zimmerer & Kottke, 1996).

On practice, RO membranes usually operate with a feed velocity that goes from 0.07 m/s to 0.20 m/s (Vrouwenvelder et al., 2011), but there are facilities that operate at higher feed velocities. The velocity inside a feed channel is never constant over time, since feed spacers create different flow velocities that vary throughout time and space along the spacers. Because of the geometrical configuration of the feed spacers, e.g., the diameters of the filaments in the spacer, the shape of the filaments, the angles formed by the intersection of the filaments, the pattern of the filaments overlaid to each other (Da Costa et al., 1994), etc., velocities vary at different locations of the spacers. Low-velocity zones along the feed spacers have been reported to be zones suitable for particulate deposition because of a lower turbulence and shear stress, thus, contributing to the perfect conditions for biofilm growth (Koo et al., 2015; Subramani & Hoek, 2008). These low-velocity zones also happen to have low variations of velocity through time, consequently having a poor disruption of the concentration polarization layer, and finally promoting scaling (Haidari et al., 2016). Another study also proved that scaling and other types of fouling are a direct consequence of low cross-flow velocities in the feed channel, because such velocities increase the concentration polarization and lower the shear stress on the surface of the membrane (Bucs et al., 2013).

Figure 9, obtained from a scientific article by (Haidari et al., 2016), explains the different crossflow velocity zones on one cell of a zigzag spacer. The cell is the enclosed area by the intersection of four spacer filaments seen from above, as shown on Figure 10.

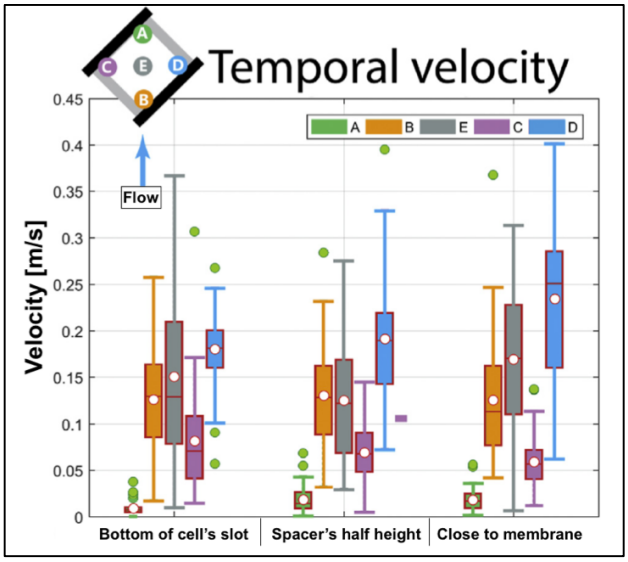


**Figure 9: Image obtained from** (Haidari et al., 2016). **Variation of crossflow velocities on a certain time frame. The velocities were measured at five different points of a zigzag spacer (point A-E), on three different heights of the spacer.**

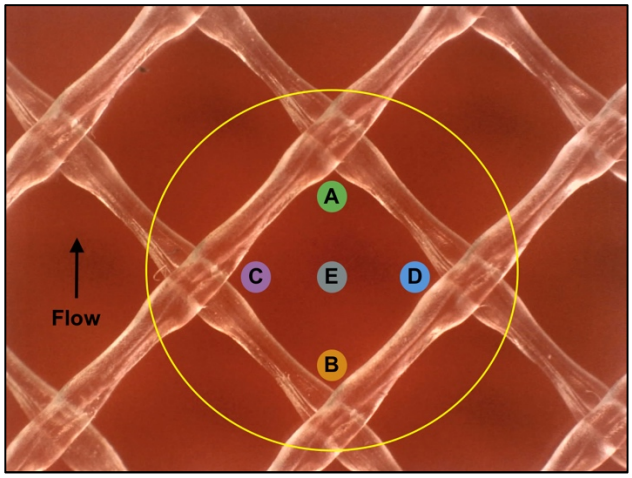


**Figure 10: The yellow circle encloses a spacer's cell. Letter A to E show the different points where the crossflow velocities were measured. The five points were measured on three different planes: (1) at the border of the spacer with the flow cell, (2) at half the height of the spacer, and at (3) the border of the spacer with the membrane. Image modified from** (Haidari, 2017).

From Figure 9, point B in the spacer's cell proves that low-velocity areas with a low velocity variation throughout time, do exist. However, Haidari's et al. study (2016) did not have permeation on the crossflow cell used. Permeation has a drag effect for particulate fouling towards the membrane surface, making a significant difference to a non-permeating flow cell. From Haidari's et al. study (2016), a more detailed correlation of low-velocity zones with particle deposition and particulate fouling could be further explained if permeation had been a possibility.

Low velocities occurring on a feed channel are not the only effect caused by the different aspects that constitutes a spacer. One particular aspect of the spacers has been found to be strongly related to the mass transfer and pressure drop in the feed channel, and that is the hydrodynamic angle θ (Da Costa et al., 1994), as shown on Figure 11. The hydrodynamic angle is described by Da Costa et al. as "*the angle between two filaments facing the feed channel axis and describes the change in direction of the fluid as it flows along the channel*".

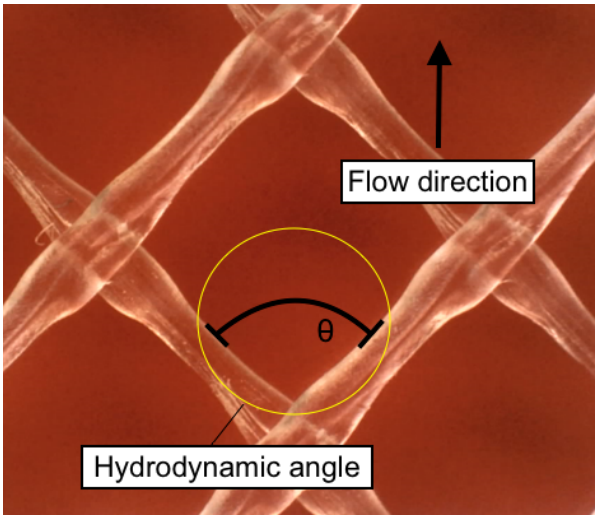


**Figure 11: Hydrodynamic angle in a zigzag spacer.**

According to Da Costa et al., when the hydrodynamic angle is increased, the pressure drop increases too due to higher energy dissipation when the flow direction is changed so extremely, as illustrated on Figure 12, therefore lower hydrodynamic angles would theoretically be preferred. Nevertheless, hydrodynamic angles less than 90°, despite of their lower pressure drop, they induce a much lower mass transfer. Hydrodynamic angles of 90° proved to achieve the highest mass transfer (Da Costa et al., 1994).

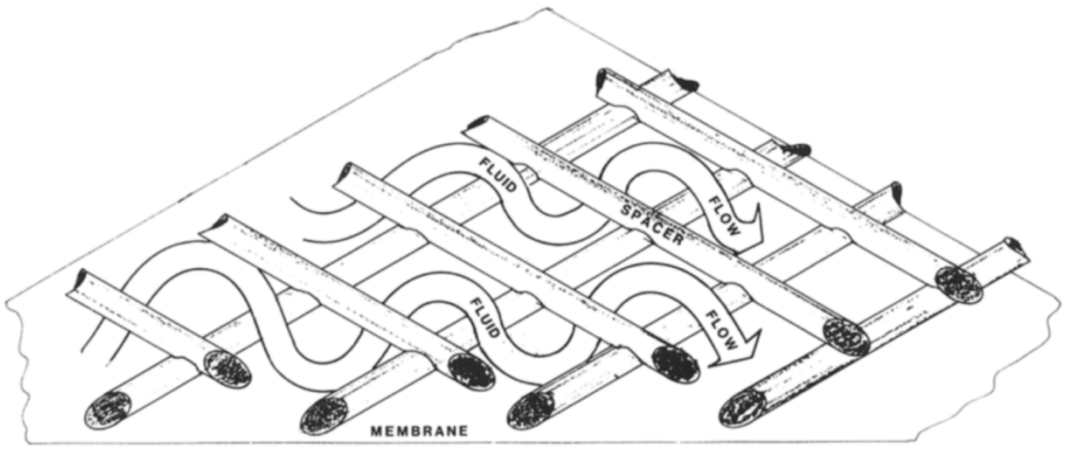


**Figure 12: Flow trajectories going through a zigzag spacer. Image obtained from** (Da Costa et al., 1994)**.**

The geometrical configuration of the different feed spacers commercially available worldwide, as well as the diverse composition of the different waters currently treated by RO membranes, have made research to start experimenting more on feed spacers. The big challenge being faced now, is to find a balance between the pressure drop and the mass transfer improvement that the geometrical configuration of the spacer can offer, considering the costs that would be implied in the production of such modified spacers, and how the implementation of these would affect the operational costs on an RO facility.

## 2.4 Mass Transfer Coefficient

The Mass Transfer Coefficient (MTC) is a key performance indicator used for monitoring how well an RO facility is operating in terms of permeate production. The MTC can notify basically two things, (1) when a membrane is suffering from any type of fouling or physical blockage that decreases the permeate flux obtained per unit of driving pressure available, or the opposite, (2) when the membrane is damaged and has a tear/leak, increasing the permeate flux and very probably worsening the permeate quality.

The MTC can be graphed when data series are obtained from an operating membrane. MTC graphs from full-scale RO facilities, usually show a negative slope, meaning that the permeate flux per unit of available driving pressure is decreasing, in other words, the membrane is fouling. On the other hand, MTC graphs which show a positive slope, mean that the permeate flux per unit of available driving pressure is increasing, implying that the membrane has a

tear/leak. Equation 1 has been used for graphing each value measured during the operation of the RO system (Gonzalez, 2017).

$$MTC = 0.55 \times \frac{Flux}{NDP} \times TCF = 0.55 \times \frac{LMH}{\frac{P_f + P_c}{2} - P_p - \pi_{f-c}} \times TCF$$

**Equation 1**

As seen on Equation 1, the MTC formula is composed of several variables that were measured over time in the experimental runs of **the Project**, for time steps of 1, 2, 5, 10 and 15 minutes. First, the permeate flux was calculated for each time step by measuring the permeate flow [L/h], and dividing it by the active area [$m^2$] of the flat-sheet membrane used.

Secondly, the Net Driving Pressure (NDP) was calculated for each time step with the average of the feed pressure [bar] and the concentrate pressure [bar] (both pressures are assumed equal since the pressure drop in the crossflow cell is very low and can be neglected) minus the pressure in the permeate [bar] (which is considered as atmospheric pressure at sea level) minus the osmotic pressure in the feed-concentrate [bar]. The osmotic pressure is calculated by multiplying the result obtained from subtracting the electrical conductivity in the feed [µS/cm] minus the electrical conductivity in the permeate [µS/cm], times 0.000318 (Gonzalez, 2017). For this last step, we assume that the electrical conductivity in the feed and in the concentrate are equal, since the relatively small size of the flat-sheet membrane does not experience concentration changes over itself.

Thirdly, the product of dividing the permeate flux over the NDP is multiplied by a Temperature Correction Factor for each time step, which is calculated as shown on Equation 2, where T is the measured temperature [°C ] at a certain time step, and the coefficient 3020 is a constant value used for water temperatures equal or less than 25 °C (DOW, 2013). For **the Project**, water temperatures were on average in the range of 20-25 °C.

The TCF basically normalizes the MTC calculation to a desired value due to the effect of viscosity that varies according to the water temperature, and for this study, the TCF corrects for a temperature of 25 °C.

$$TCF = exp\left(3020 \times \left(\frac{1}{T+273.15} - \frac{1}{298.15}\right)\right)$$

**Equation 2**

Finally, the coefficient 0.55 in Equation 1 is empirically proposed and used in order to unitize the MTC values of each time step, e.g., 1.15, 1.00, 0.925. The coefficient 0.55 is different according to the permeate flux used and the NDP, factors which depend on the type of water to be treated and the operating conditions set for the RO facility being studied (Gonzalez, 2017). This coefficient can be selected by trial-and-error.

# 3. MATERIALS AND METHODOLOGY

## 3.1 AnMBR operation and maintenance

Operating and maintaining the lab-scale AnMBR located at **Biothane's** laboratory was also part of **the Project,** being a parallel and complementary activity to the RO experiments, but it is not in the objective of this study. Obtaining stable conditions in the reactor was crucial in order to get constant characteristics in the effluent. The more constant the AnMBR's permeate quality, the more consistent the results obtained from the experiments done on the RO system. This could be achieved successfully.

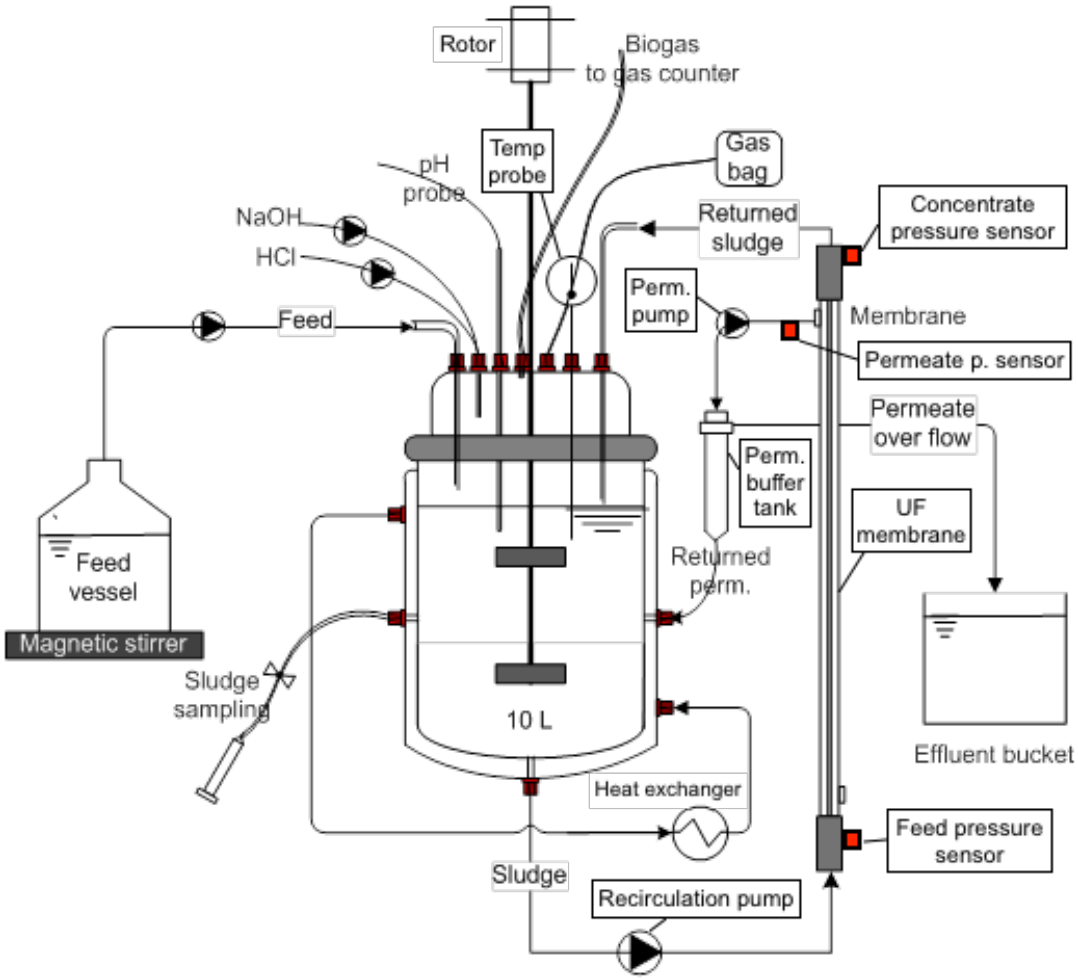


**Figure 13: Scheme of the actual AnMBR for PTA wastewater treatment. The scheme was courtesy of Biothane-Veolia.**

The AnMBR was fully controlled and monitored by a programmable logic controller (PLC): feed pump, permeate pump, acid and caustic dosing pumps, recirculation pump, and reactor's

levelling pump. The computer registered all the parameters measured from the AnMBR, such as membrane pressures, reactor's temperature, reactor's pH, biogas production, among others.

### 3.1.1 Analyses

The analytic section of the laboratory carried out the following analyses:

**Table 1: AnMBR's permeate and feed analyses**

| Source | Analysis | Unit | Frequency per week |
|---|---|---|---|
| Permeate | COD | mg/L | Twice |
| | Volatile Fatty Acids (VFA) | mg/L | Twice |
| | Total Phosphate | mg/L | Once |
| | Alkalinity ($HCO_3^-$) | meq/L | Once |
| | Total Kjeldahl Nitrogen (TKN) | mg/L | Once |
| | Ammonium | mg/L | Once |
| Feed | COD | mg/L | Twice |

### 3.1.2 Data-log

A data-log was carried out daily, capturing the following parameters from which some were read from the computer's PLC:

- Feed consumed over a day [L]
- MLSS temperature [°C]
- MLSS pH
- Reactor`s volume [L]
- Biogas production [L/day]
- Membrane feed pressure [mbar]
- Membrane concentrate pressure [mbar]
- Permeate side pressure [mbar]
- TMP [mbar]
- Acid and caustic dossing [mL/day]
- LMH (liters per square meter per hour)
- Biogas' methane fraction [%]

The daily data-log was later captured in an excel sheet in order to graph the most relevant parameters for monitoring the performance of the AnMBR. The graphed parameters had a daily development, which helped notice any abnormality in the AnMBR. The most important graphed parameters were:

- Transmembrane pressure (TMP)
- COD removal
- COD balance
- VFA concentration in the permeate
- Volumetric Loading Rate (VLR)

Other manual activities on the AnMBR were done on a weekly basis: preparing the PTA wastewater synthetically. Activities done on a monthly basis: (a) replacing the feed and permeate pump tubings, (b) changing the permeate overflow line when clogged, and (c) greasing the rotor to avoid biogas leaks.

### 3.1.3 Cleaning in Place

Cleaning in place (CIP) of the membrane was carried out every 5 to 6 weeks, when the TMP was too high for its standard operating values. For this activity, the methodology recommended by the membrane manufacturer was followed. First, the membrane was emptied and flushed with normal water in order to create shear forces on the membrane walls that could remove fouling. After this, the membrane was soaked for one hour with a basic solution, composed of sodium hypochlorite and potassium hydroxide. Next, the membrane was again flushed with normal water, and an acid solution composed of citric acid was introduced, letting the membrane soak for another hour. Lastly, the membrane was once again flushed with normal water, pH was checked in order to be sure that no acidity was remaining in the membrane. Posterior to this, the membrane was again put in "sludge recirculation mode".
Considering all the aforementioned activities, the importance of a well operated and maintained AnMBR reactor is restated.

## 3.2 AnMBR permeate

One of the crucial elements required in **the Project** was the feed water for the RO system, since it naturally had the properties that could eventually induce fouling, e.g., dissolved organic matter, dissolved salts, etc. The RO-feed is the AnMBR-permeate. The origin of the AnMBR-permeate is wastewater discharged from the production of purified terephthalic acid (PTA), which in **the Project's** case, it is synthetized at **Biothane's** laboratory.

PTA is the main raw material for the production of polyester fibres for the textile industry, polyethylene terephthalate (PET) bottles and polyester films for audio-visual, photographic, computational, packaging applications, among some other ones that represent a much smaller consumption in the worldwide production of PTA (Macarie et al., 1992). The four main organic compounds that compose PTA wastewater are terephthalic acid, benzoic acid, para-toluic acid (p-toluic acid) and acetic acid, which can represent on average 80-95% of the total COD

concentration (Kleerebezem, 1999b). Moreover, it is presumed that PTA acts as a mutagen (Thiruvenkatachari et al., 2007), a carcinogen and it might be linked to the sperm quality in animal species (Kleerebezem, 1999a). In other words, discharging PTA wastewaters and PTA by-products into the environment is toxic for humans and animals (Karthik et al., 2008). Thus, the increasing interest of researchers in the treatment of PTA wastewaters.

The RO-feed, which had been previously filtered through a UF membrane in the AnMBR, should contain almost no suspended solids, since the UF membrane nominal pore size is 0.03 microns, which in theory is able to remove the majority of colloidal particles, bacteria and larger viruses, as well as more than 99% of all suspended matter (van Halem et al., 2009a). This would mean that basically smaller colloids and dissolved matter is passing through the UF membrane, implying that the RO-feed would not contain suspended particles. However, by doing a "particle counting" at TU Delft's water laboratory, it was found that particles bigger than the UF membrane nominal pore size were present in the AnMBR permeate. Fouling on the RO membrane is expected due to the presence of bigger particles as shown on Figure 14.

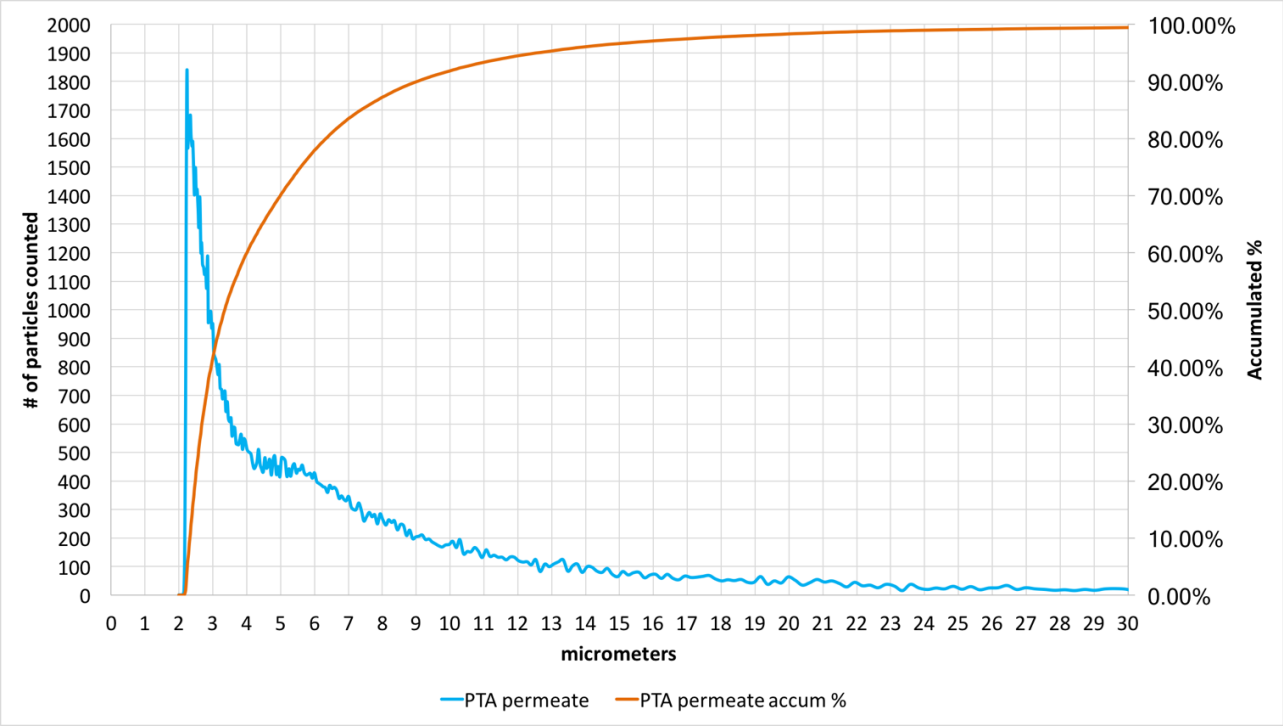


**Figure 14: Particle counting for the AnMBR permeate is represented by the blue line. The orange line represents the particle counting accumulated percentage.**

The PhD study by Lousada-Ferreira (2011) describes the increment in particle size on the permeate side of the membrane of MBRs. This phenomenon can be attributed to a membrane leakage or a physical/(bio)chemical process that could be happening on the membrane itself or on the permeate side of the membrane system, such as nucleation and further crystallization,

as well as aggregation by particle destabilization. Moreover, backwashing the MBR's membrane with chemicals is known to cause a particle growth within a size range of 2-5 micrometers (Lousada-Ferreira, 2011a).

The AnMBR-permeate was collected on an air-sealed 15 liter vessel. The AnMBR-permeate collection vessel needed to be air-sealed since the AnMBR-permeate is naturally anaerobic (no electron acceptors present in the medium) and no oxygen is wanted to dissolve into the permeate, otherwise the anaerobic conditions wouldn't be met; however, no anaerobic conditions could be achieved. Dissolved oxygen was detected on very low concentrations, around 2 mg/L, this due to an air opening connected to the AnMBR-permeate buffer tank that serves as a pressure equalizer for the reactor's inner pressure, as well as a permeate collection point.

The AnMBR permeate collection vessel has three main hoses that were sealed to the lid and enter into the vessel as shown on Figure 15.

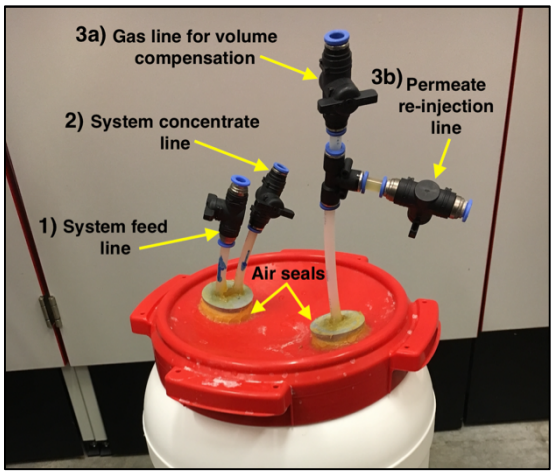


**Figure 15: RO feed vessel, (1) one long hose that reaches the bottom of the collection vessel so that all the AnMBR permeate collected, also called the RO feed, can be sucked by the RO pump; (2) one shorter hose that returns the concentrate back into the collection vessel; and (3a) one hose connected to a gas bag that only serves for compensating the changes in volume inside the vessel when RO permeate is being produced. There is also an additional connection to the gas line, a (3b) permeate re-injection line that serves for dosing back the RO permeate at the rate it is being produced, this in order to maintain the same ion concentration in the feed.**

## 3.3 RO System

All of the RO system was supplied by Sterlitech, an American company based in Kent, Washington, USA. The pump, the valves, the manometers, flowmeters, flat-sheet membranes and crossflow cell were supplied by Sterlitech. The feed spacers and the differential flow meter were supplied by Dr. Amir Haidari, TU Delft section of Sanitary Engineering. The portable multi-parameter meter was supplied by the Water Laboratory at TU Delft's faculty of Civil Engineering. Figure 16 shows a representative scheme of the assembled RO system.

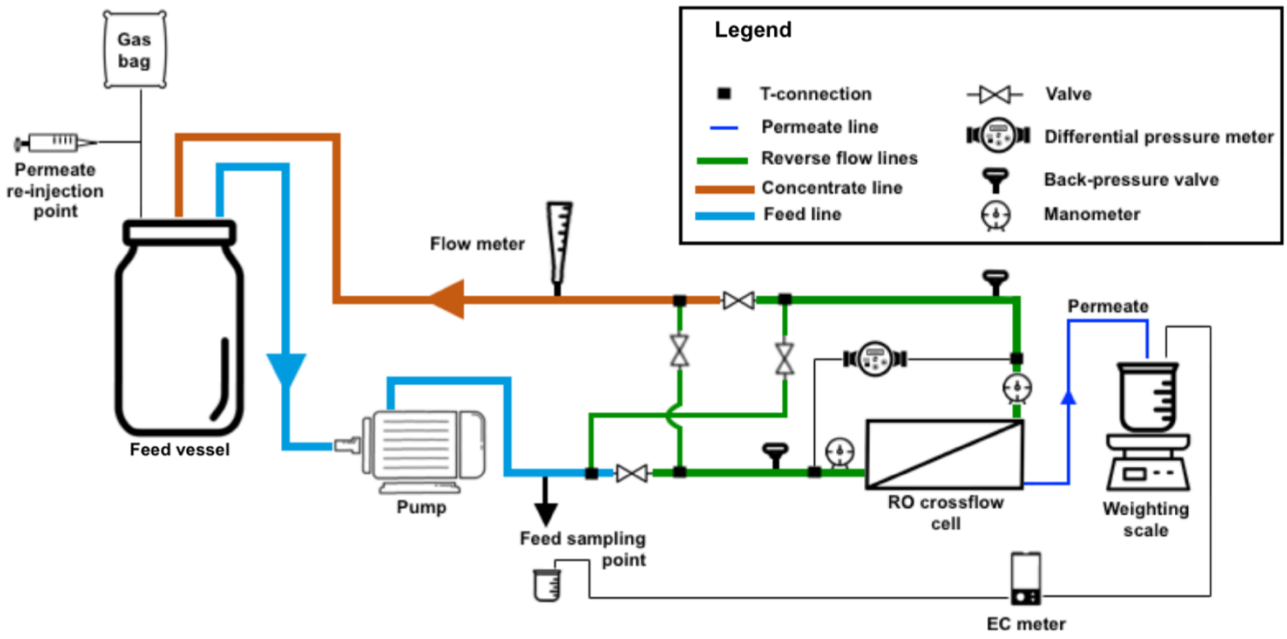


**Figure 16: RO system scheme**

### 3.3.1 RO crossflow cell

A full-scale RO element was not used as an experimental set-up for **the Project**, even though very good results can be obtained from it. The crossflow cell used was a much cheaper solution and more practical, occupying less space and being easier to operate compared to a full-scale RO element. The crossflow cell specifications are shown in Table 2.

**Table 2: RO Crossflow cell specifications.**

| Parameter | Value |
|---|---|
| Membrane active area | 42 $cm^3$ |
| Membrane active length | 9.207 cm |
| Membrane active width | 4.572 cm |
| Crossflow cell max pressure | 69 bars |
| Crossflow cell max. Temp | 150 °C |
| Feed channel depth | 2.28 mm |
| Feed channel width | 39 mm |

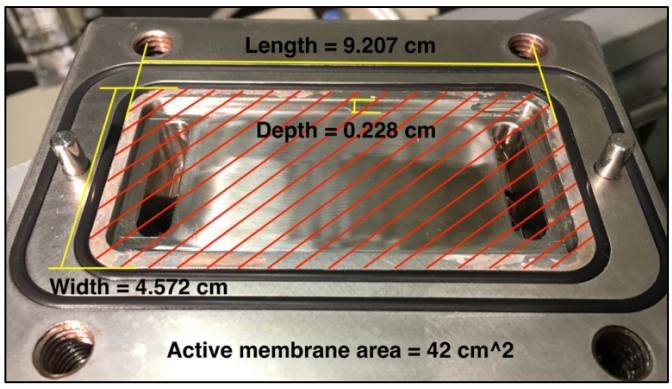


**Figure 17: Active membrane dimensions of the RO crossflow cell. The red lines mark the active membrane area. The depth is the height of the feed channel.**

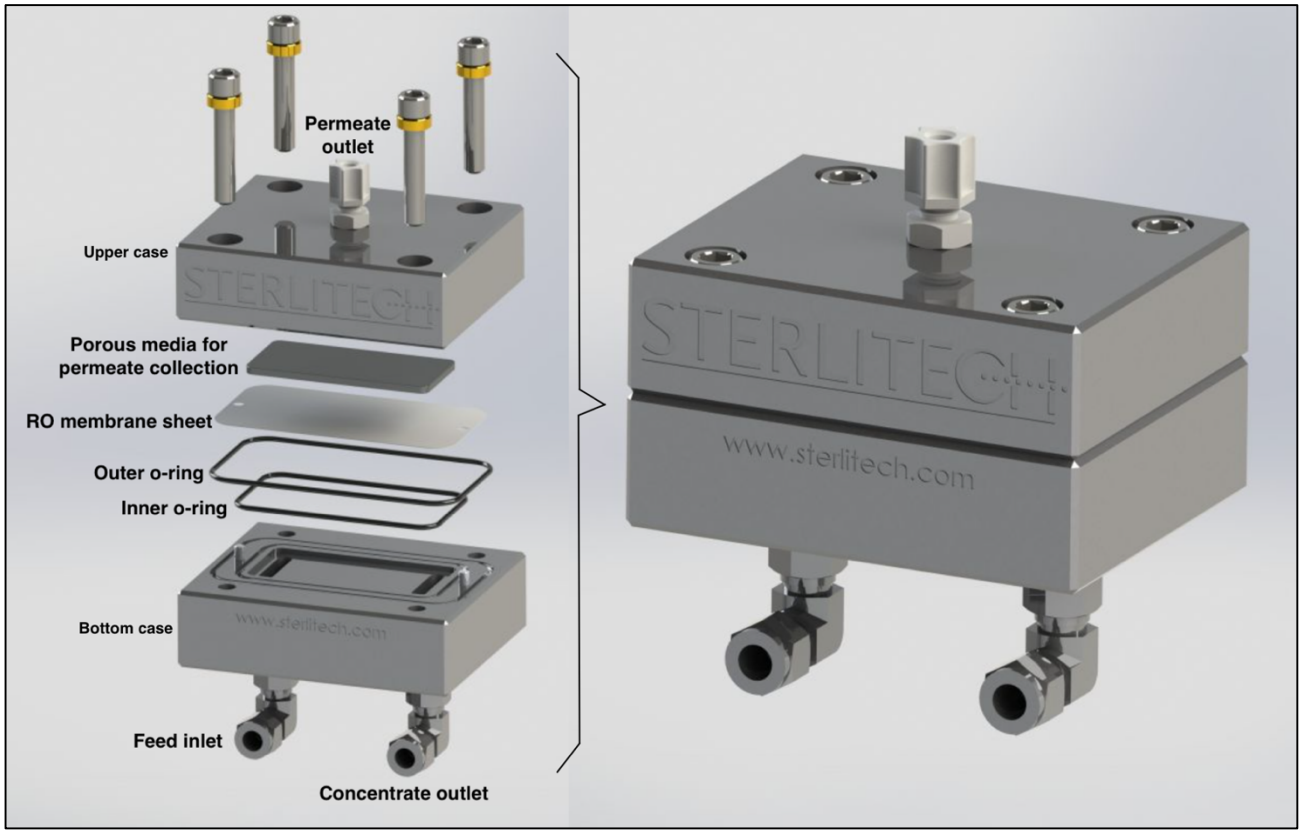


**Figure 18: RO crossflow cell assembly. Image modified from** (Sterlitech, 2017)

Figure 18 shows the assembly of the crossflow cell and the parts that compose it. The cell is able to produce permeate, which is essential for graphing the mass transfer development over time. The feed spacer lies between the RO flat-sheet membrane and the bottom case of the crossflow cell, fitting right in the cavity inside the inner O-ring, as shown on Figure 20.

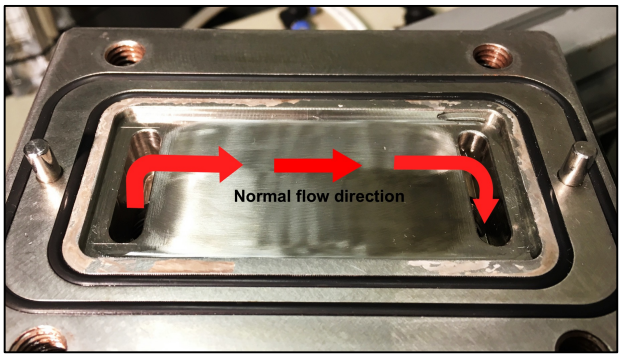


**Figure 19: The red arrows indicate the normal direction of the feed flow in the feed channel.**

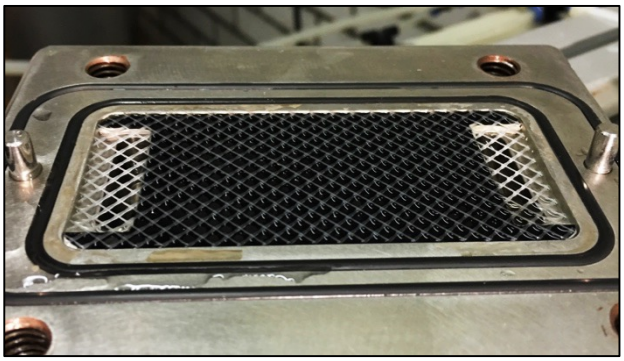

**Figure 20: Feed spacer placed. A black plastic shim can be seen beneath the spacer. It held in place the spacer inside the feed channel.**

### 3.3.2 Feed spacers

Two different feed spacers were used in **the Project**, a zigzag spacer (Figure 21) and a cavity spacer (Figure 22). The specifications of each spacer are shown in Table 3

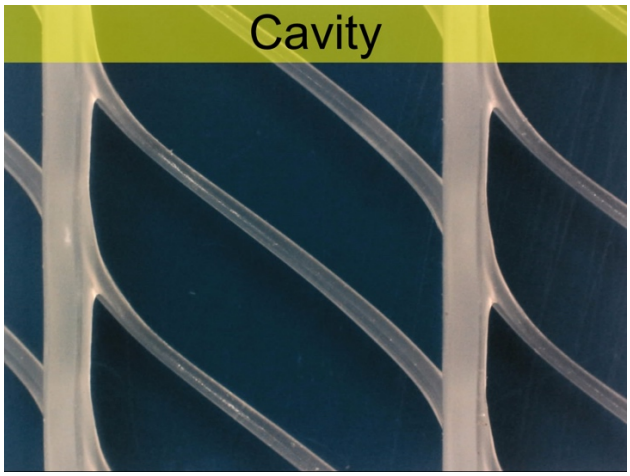


**Figure 21: Cavity spacer used in Run 1 and 2 of the final phase of experiments. Image modified from** (Haidari, 2017).

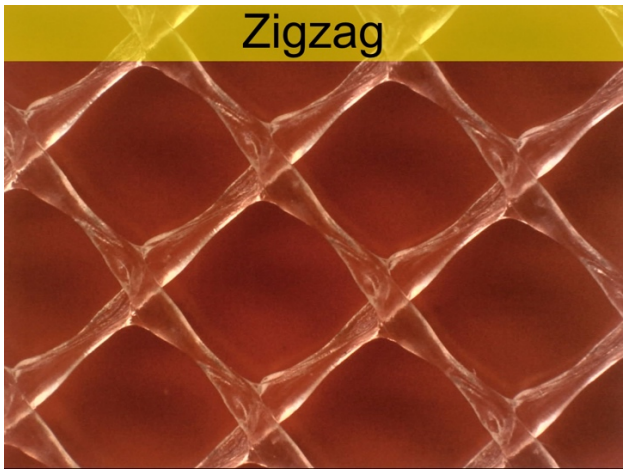


**Figure 22: Zigzag spacer used in Run 3 and 4 of the final phase of experiments. Image modified from** (Haidari, 2017).

**Table 3: Feed spacers relevant specifications. The height of the spacer corresponds to the height of the feed channel inside the crossflow cell. The porosity is a parameter used for the calculation of the crossflow velocity.**

| | Units | Cavity spacer | Zigzag spacer |
|---|---|---|---|
| Spacer/Channel height | mm (mil) | 0.71 (28) | 1.25 (49) |
| Porosity | % | 88 | 82 |
| Hydrodynamic angle θ | ° | 89.5 | 45 |

A disadvantage of the RO crossflow cell is that the feed channel height is overdimensioned, with a height of 2.28 mm, being three times higher than the zigzag spacer and almost two times higher than the cavity spacer used in this study. This means that both spacers would be loose inside the feed channel, and their function, flow mixing and disruption of concentration polarization layer, wouldn't be satisfied, as shown on Figure 23.

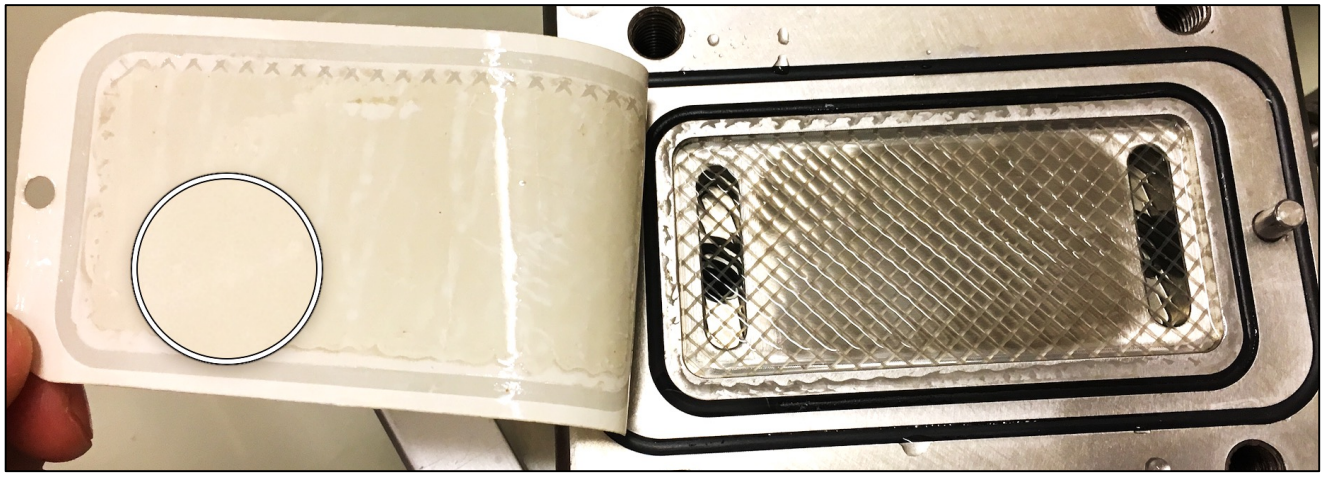

**Figure 23: On the right side of the image, crossflow cell with a zigzag spacer and no plastic shim. On the left side, a fouled flat-sheet membrane. The circle on the membrane is a zoomed-in area, showing a homogeneous fouling, proving that the spacer did not comply with its functions.**

The solution to the overdimensioned feed channel height was to place plastic shims inside the feed channel in order to meet the required spacer height. Two shims with different thicknesses were used, a black shim and a white shim shown on Figure 24. The plastic shims were measured with a vernier caliper for the best accuracy. Combinations of the plastic shims were done for fitting the required channel height for each of the two spacers. After this, the shims could be cut out to fit the feed channel.

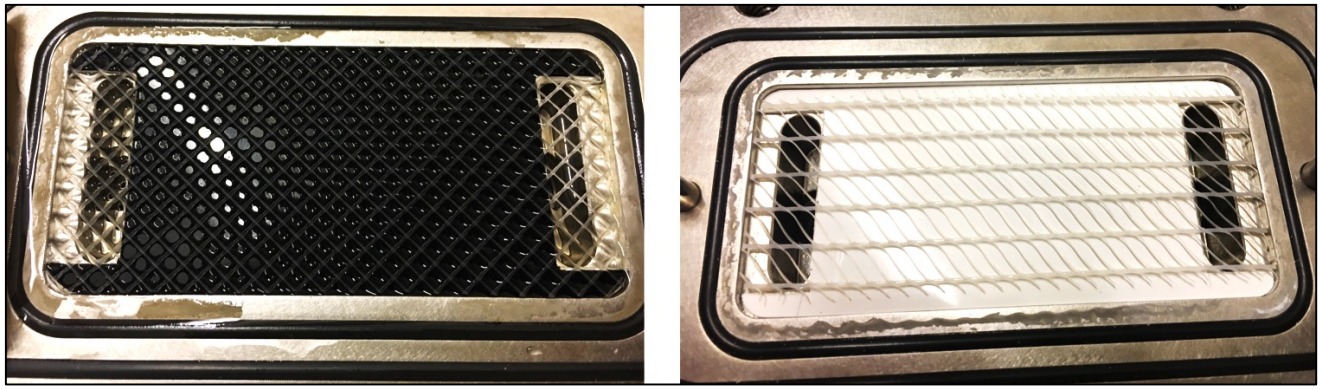

**Figure 24: Black and white shims used.**

Having made the feed channel height to coincide with the spacer height, the crossflow velocity [m/s], inside the feed channel could be calculated with Equation 3, where $Q$ is the feed flow [$m^3/s$], $A$ is the channel cross-section area [$m^2$], and $\rho$ is the spacer porosity (Haidari, 2017).

$$Crossflow\ velocity = Q/(A \times \rho)$$

**Equation 3**

### 3.3.3 RO flat-sheet membrane

The flat-sheet membranes were manufactured by The Dow Chemical Company, and supplied by Sterlitech Corporation. The membranes had an active area of 42 $cm^2$. The membrane code is BW30XFR-400/34 (Brackish Water, Fouling Resistant). Membrane specifications are shown next (Table 4).

**Table 4: Flat-sheet membrane specifications, obtained and modified from** (DOW, 2016).

| | |
|---|---|
| Max. Operating temperature | 45 °C |
| Max. Operating Pressure | 41 bar |
| pH range, continuous operation | 2-11 |
| pH range, short-term cleaning (30 min.) | 1-13 |
| Max. Feed Silt Density Index (SDI) | 5 |
| Free chlorine tolerance | < 0.1 ppm |
| Active membrane area | 42 $cm^2$ |
| Typical stabilized salt rejection** | 99.65% |

**Based on the following conditions: 2000 ppm NaCl, 15.5 bar as feed pressure, 25 C water temp.

## 3.4 Preparatory phase of experiments

A preparatory phase of experiments was carried out in order to gain more insight into the operation of the RO system, as well as achieving the desired RO feed concentration for accelerating the fouling process for the final phase of experiments. This preparatory phase consisted of four runs which are described on Table 5.

**Table 5: The four preparatory runs with their respective characteristics**

| Run | Spacer type | Spacer/channel height [mm] | Feed concentration | Initial EC [mS/cm] | Final EC [mS/cm] | EC concentration factor | Run duration |
|---|---|---|---|---|---|---|---|
| A | Zigzag | 0.71 | Increasing | 8.20 | 8.67 | 1.057 | 230 mins |
| B | Zigzag | 0.71 | Constant | 8.36 | 8.42 | 1.007 | 230 mins |
| C | Cavity | 1.25 | Increasing | 7.68 | 14.70 | 1.914 | 5 days |
| D | Zigzag | 0.71 | Increasing | 7.95 | 14.90 | 1.874 | 5 days |

Run C was preparatory to achieving the desired concentration for Run 1 and 2 of the final phase of experiments. Run D had the same objective as Run C, but preparatory to Run 3 and 4 of the final phase of experiments. In other words, the final concentration achieved in Run C and Run D corresponded the initial concentration for Run 1 and Run 2, and Run 3 and Run 4 respectively. The concentrations in Run 1, 2, 3 and 4 were kept constant throughout the whole runtime, just as done in Run B, which is explained in the next paragraph and illustrated in the diluting scheme on Figure 25 as well.

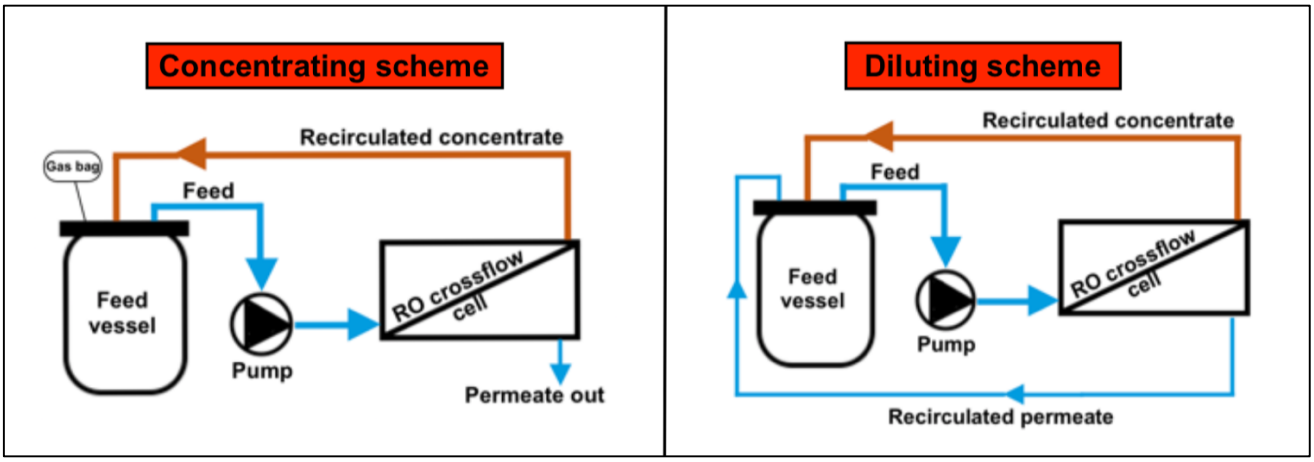


**Figure 25: Operating schemes for the experiments. Run A, C and D operated under the concentrating scheme, and Run B under the diluting scheme.**

In order to achieve a constant concentration of salts in the feed during Run B, demineralized water was introduced back into the RO feed vessel at the same rate as the permeate production, as shown in the diluting scheme shown on Figure 25, allowing the salts concentration to remain relatively equal, therefore keeping a constant osmotic pressure. Having a constant osmotic pressure over time can be interpreted as having a non-changing concentration polarization effect, which means that any decrease in the mass transfer is not attributed to the concentration polarization, but to fouling. The MTC development over time for a constant concentration of salts in the feed was graphed, as well as the one for an increasing concentration of salts, as shown on
Figure 27 and Figure 26 respectively.

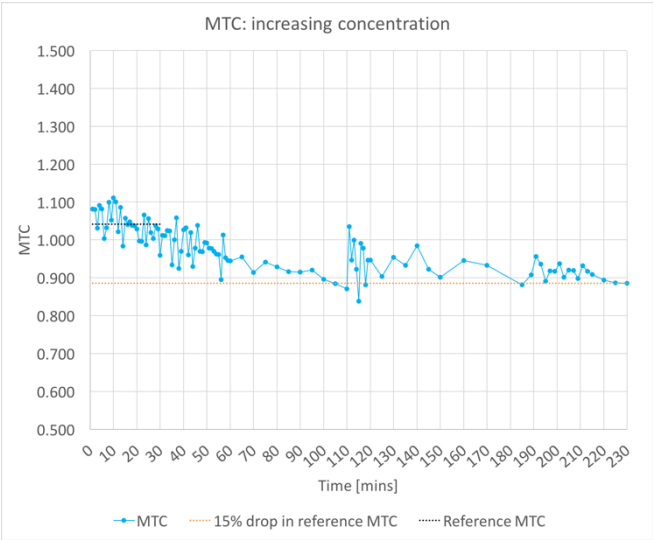


**Figure 26: MTC development for Run A surpasses the orange dotted line, which represents the threshold of 15% drop in the reference MTC value, the black dotted line, after minute 100 and minute 180.**

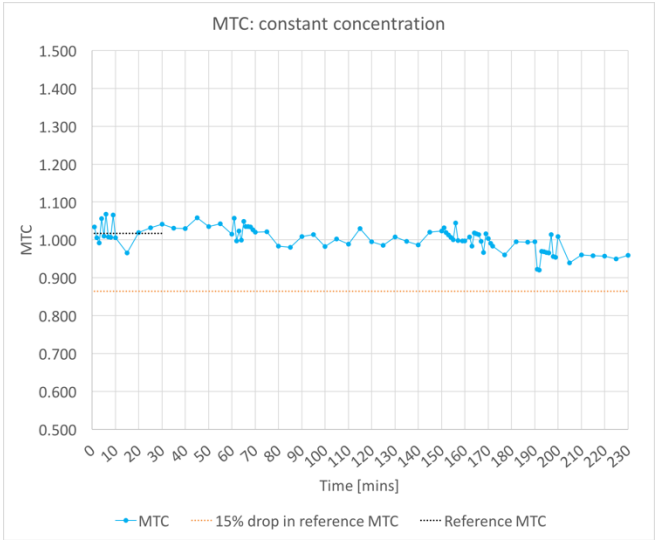


**Figure 27: MTC development for Run B, stays relatively constant compared to the MTC from Run A, because the concentration polarization layer remained constant. After minute 170 (second day of operation), a decrease in the MTC line can be observed, which means fouling.**

As seen on Figure 26 and Figure 27, a 15% drop on the reference MTC value was chosen. The motivation for this threshold was because it is usually a common value used on full-scale RO facilities (Bucs et al., 2014). Usually, when MTC drops beyond a 15% from the reference MTC value, the membrane integrity cannot be recovered by a CIP, in other words, irreversible fouling occurs. A negative slope on a graphed MTC means that the permeate flux produced per unit of available driving pressure is decreasing over time.

From Run A and B, it was concluded that the gradual increase in concentration polarization in Figure 26 had a much higher and quicker effect in the MTC development than the effect of fouling alone shown in Figure 27. However, the effect of fouling alone in Run A cannot be differentiated from the effect of an increasing concentration polarization effect in the same Run. For this reason, the final phase of experiments was decided to be done with a constant feed water concentration.

## 3.5 Final phase of experiments

The main objective of this phase of experiments was to observe the effect of crossflow reversal on the fouling removal, expressed in terms of mass transfer, for the two different feed spacers used in **the Project**.

The final phase of experiments consisted of four different runs on the RO system shown in Table 6. For every run, a new feed spacer and flat-sheet membrane was used. The flat-sheet membranes were let to soak on demineralized water at least one day before being used. The four runs followed the "diluting scheme" shown on Figure 25, meaning that the feed concentration in each run was kept constant throughout time.

**Table 6: Four runs and their corresponding specifications.**

| Run | Spacer type | Spacer/channel height [mm] | Average feed EC [mS/cm] | Crossflow reversal frequency | Average crossflow velocity [m/s] | Average permeate flux [LMH] |
|---|---|---|---|---|---|---|
| 1 | Cavity | 1.25 | 14.70 | After the fifth day | 0.362 | 20 |
| 2 | Cavity | 1.25 | 14.98 | Twice-a-day | 0.367 | 20 |
| 3 | Zigzag | 0.71 | 14.90 | After the fifth day | 0.361 | 20 |
| 4 | Zigzag | 0.71 | 14.95 | Twice-a-day | 0.364 | 20 |

The average crossflow velocity of the four runs was 0.36 m/s, which is slightly higher than the maximum velocity used in full-scale RO facilities. The main reason for this was because the RO system was not capable of adjusting the crossflow velocity to a lower velocity. The pump used was operated by a frequency meter that was close to the limit. The RO system supplier recommended not to operate the pump at low frequencies. However, 0.36 m/s is an optimistic crossflow velocity for fouling removal, since it promotes a wider range of variations in velocities, and consequently, a better flow mixing (Haidari et al., 2016). This was expected to enhance fouling removal.

The applied feed pressure was not constant, since the RO system is not automated. Any slight movement in the back-pressure valve would change the pressure by 1 bar or more. It was a challenge to maintain relatively stable pressure and flow rate in the RO system.

The average electroconductivity (EC) for the feed in all four runs was 14.88 mS/cm. This EC value is approximately 1.9 times the AnMBR's permeate EC. Assuming a pressure vessel with six RO elements, a feed EC of 7.83 mS/cm would be 1.9 times concentrated at the exit of the sixth element, assuming a 10% permeate recovery on each element. The reasons behind choosing a concentration factor of 1.9 was because (1) it was desired to simulate the fouling effect on the sixth RO element of a full-scale pressure vessel, and also because (2) this phase of experiments could not be extended timewise, and fouling needed to be accelerated.

It's important to mention that the RO system could not be operated autonomously. This implied that the system had to be shut down after a working day at **Biothane,** and during lunch break, from 13:00 to 14:00 hours from Monday to Friday. The system was not operated on the weekends.

For each of the four runs, a feed sample was taken at the beginning and end of a continuous operation. For each sample, EC, pH, temperature, dissolved oxygen (DO) and Reduction-Oxidation (Redox) potential were measured.

For the MTC graphs, three parameters were measured on time frames of 1, 2, 5, 10 and 15 minutes depending on the feed pressure stability. A strict time frame was not necessary. These three parameters were (i) the concentrate flow, read from the flowmeter in the concentrate line; (ii) the feed pressure, read from the manometer on the feed line; and (iii) the permeate flow, calculated by weighing the permeate produced over a certain time frame. The feed temperature and EC were also crucial for MTC graphs, this is explained in detail on section 2.4

As done on the preparatory phase of experiments, and following the same motive, a 15% drop on the reference MTC value was set as irreversible fouling threshold.

# 4. RESULTS AND DISCUSSION

## 4.1 Cavity spacer

Run 1 and Run 2 used the cavity spacer. A new membrane and spacer were used at the beginning of each of the two runs. When beginning each run, the membrane was let to permeate for at least 30 minutes before starting taking measurements. This would ensure that the membrane acclimatizes to the operating conditions of the system. As mentioned in the previous section, the operating permeate flux for Run 1 and 2 was on average 20 LMH.

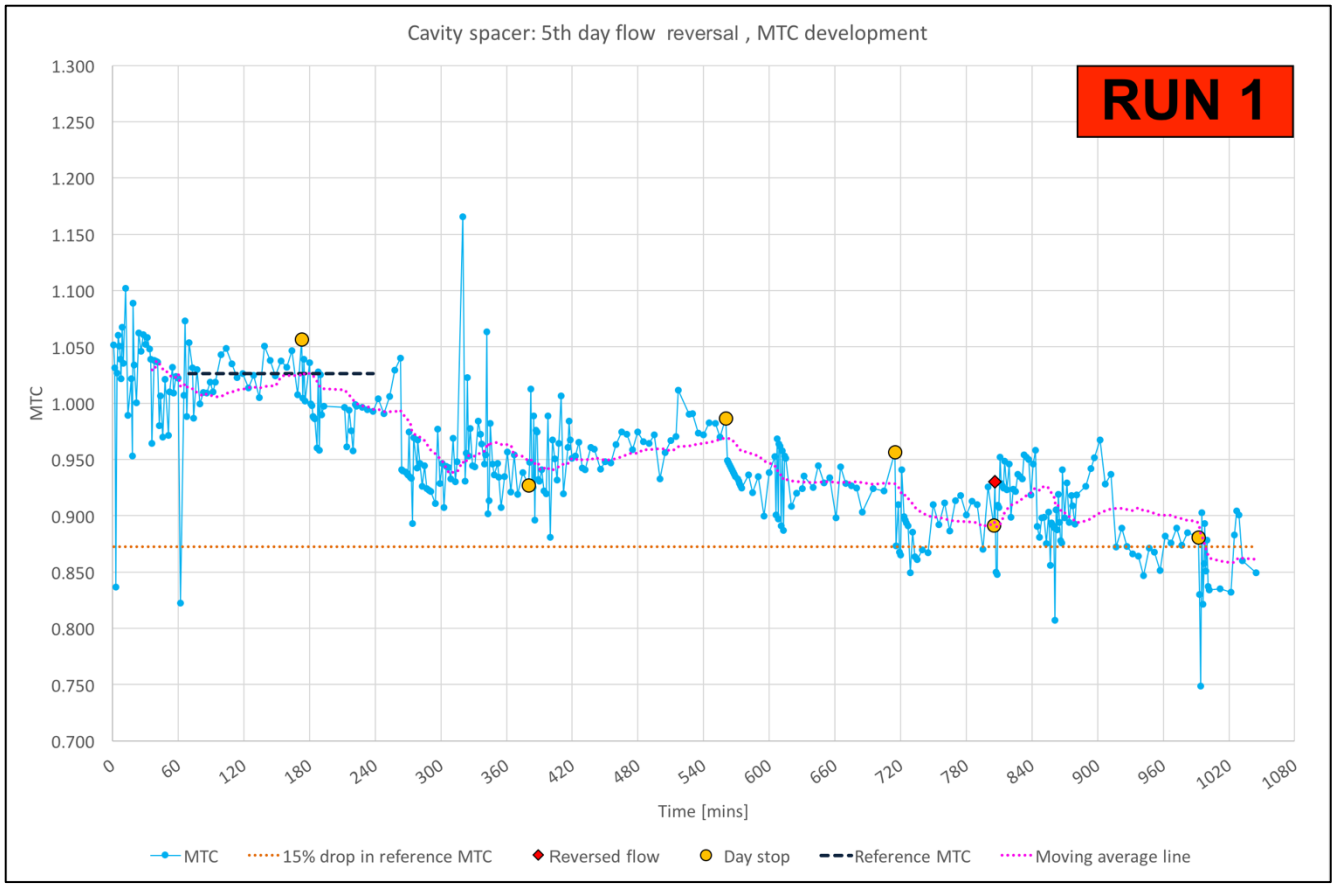


**Figure 28: MTC development for the cavity spacer when reversing the flow direction after the fifth day. This experiment was run for approximately 1045 minutes with daily stops.**

An insight into Figure 28: The yellow circles show when a daily run on the RO system was over. The red square represents the minute on which crossflow reversal was done, which for this case corresponds to the beginning of the sixth day (minute 806). The black dotted line (reference MTC) is the average MTC value corresponding the conditions of a clean membrane and spacer. The orange dotted line means a 15% drop on the reference MTC. The pink dotted line is the moving average of the blue graph, allowing it to show a clearer trend on the MTC. The x-axis shows the runtime on the membrane, not the real time, e.g. the first day had a runtime of approximately 180 minutes, even though a day consists of 1440 minutes. The runtime criterion is the same for all four runs of the final phase of experiments.

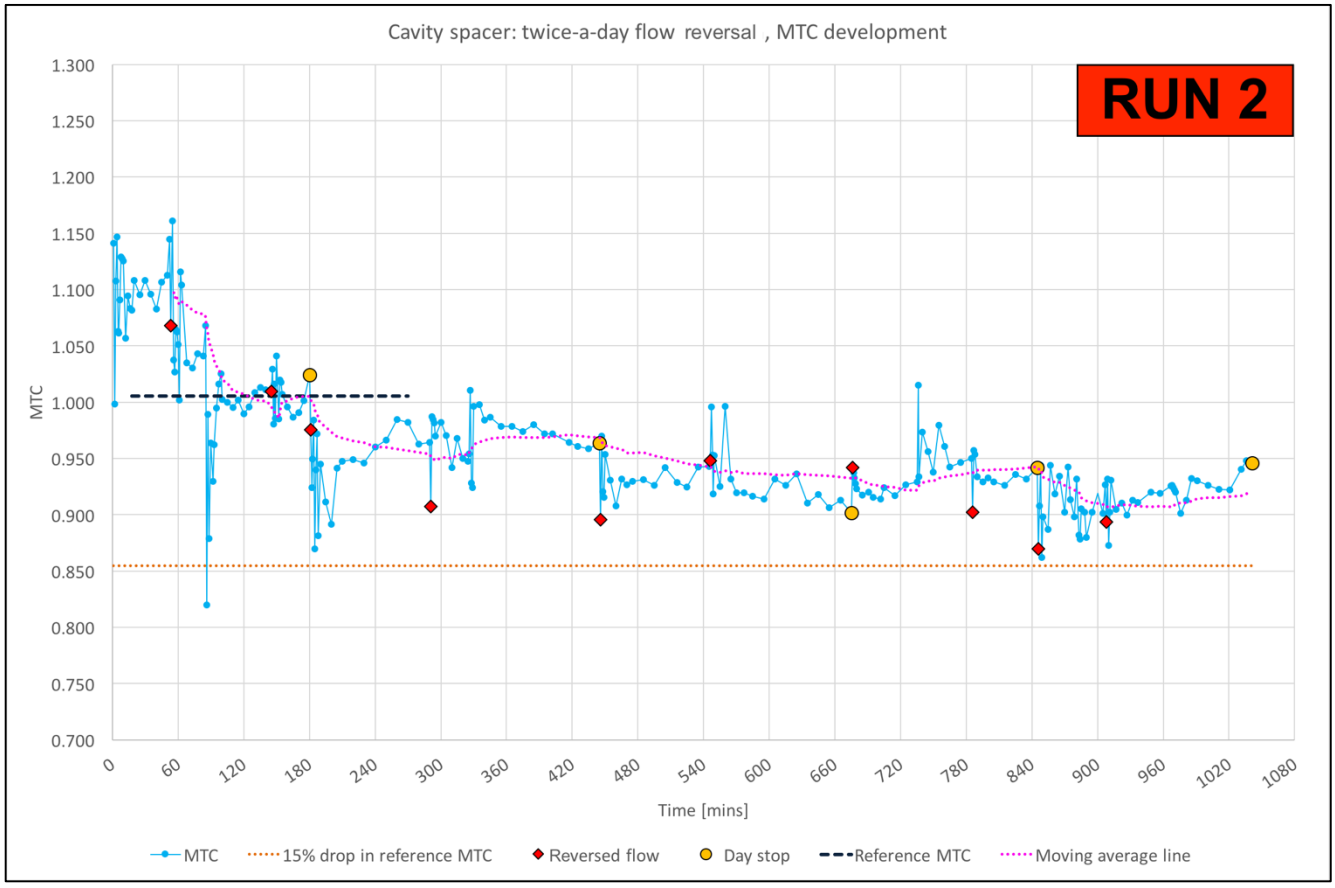


**Figure 29: MTC development for the cavity spacer when reversing the flow direction twice a day. This experiment was run for approximately 1041 minutes with daily stops. The red squares show the minute on which crossflow reversals were done (two crossflow reversals per day for this run).**

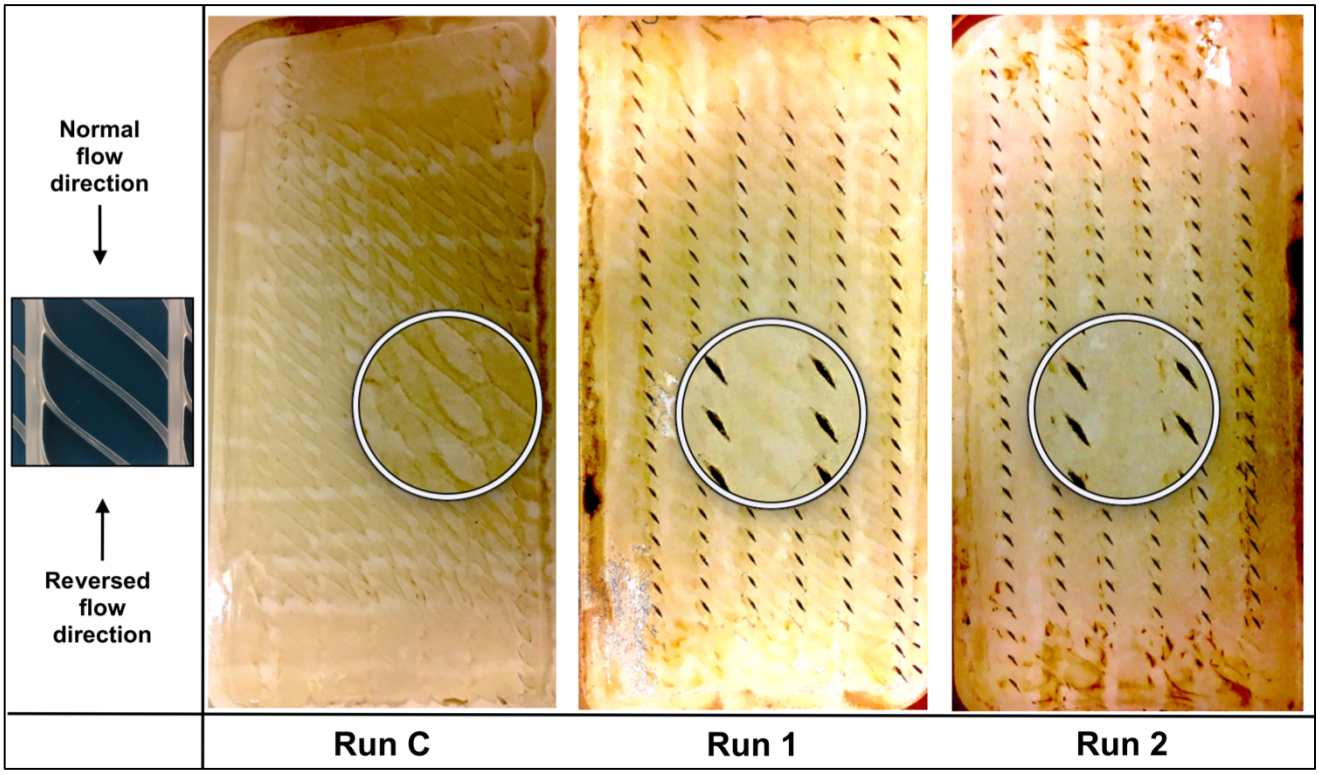


**Figure 30: Visual fouling on three different flat-sheet membranes using the cavity spacer. For each run, a new spacer and flat-sheet membrane were used. The circles on each membrane show a zoomed-in area of a well-defined fouling pattern.**

The three different flat-sheet membranes shown in Figure 30 illustrate the increased organic/particulate fouling, from left to right. Run C had no crossflow reversal, showing the sharpest fouling pattern on the membrane, however, this run cannot be compared to the other runs, since its purpose was to concentrate the feed to the desired level. Run 1 has a lighter evidence of fouling pattern compared to Run C, which is attributed to the crossflow reversal done after the fifth day of operation (minute 806). Run 2 shows no visual fouling patterns at all. The more frequent the crossflow reversal done with the cavity spacer, the more organic/particulate fouling removed from the membrane. However, a decrease on visual fouling is not a solid proof of the effectiveness of crossflow reversal on organic/particulate fouling removal.

Run 1 (Figure 28) shows that the MTC momentarily dropped below a 15% from the reference MTC on minute 720 (fourth day of operation), whereas Run 2 (Figure 29) had dropped approximately 8%. On Run 1, from minute 920 onwards, the MTC had definitely dropped a 15% from the reference MTC, reaching even a 20% drop on minute 1020, whereas Run 2 had dropped approximately a 10%. Even though a crossflow reversal was done at minute 806 on Run 1, the MTC development showed no regression. On the other hand, the MTC development on Run 2 showed a less steep drop, never reaching the 15% drop.

A negative slope on a MTC graph means that the permeate flux produced per unit of available driving pressure is decreasing. This means that Run 2 operated and ended on average with a higher permeate flux per unit of available driving pressure than Run 1. This corroborates the conclusion from the visual fouling shown on Figure 30, saying that a more frequent crossflow reversal on the cavity spacer, controls/retards fouling better over time, thus controlling/retarding mass transfer drop over time. Crossflow reversal does have a positive effect on fouling removal, it does sustain MTC for longer periods, but has no effect on MTC regression.

The MTC drop in Run 1 and 2, can be attributed to two types of fouling: (i) organic/particulate fouling, which can be removed at some extent by crossflow reversal, and (ii) scaling, which was experienced to not be removed by crossflow reversal. Even though crossflow reversal proved to remove organic/particulate fouling, the degree of removal cannot be measured by analysing a MTC development.

A localized measurement of the velocity regions, like the PhD study of Haidari (Haidari, 2017), was not done in this study, however, as concluded by Haidari (2017), from the fouling patterns shown on Figure 30, it can assumed that the darkest fouling zones correspond to the lowest crossflow velocity regions with a lower velocity variation along the spacer, and the zones without visual fouling correspond to the highest velocity regions with the highest variations. Further studies should be done on the cavity spacer in order to corroborate the previous assumption.

On the other hand, a big disadvantage of the cavity spacer is that the transverse filaments are exclusively located on one end of the height of the longitudinal filaments, leaving the other end with no filaments, as shown on Figure 31. For this study, since the feed channel was designed to permeate only from the upper side of the crossflow cell, the cavity spacer could have its effect on the mass transfer and fouling on the membrane. However, if the cavity spacer were to be applied in a spiral wound configuration, the sheet membrane that is not in contact with the transversal filaments would suffer from a totally different effect, having much less flow mixing and concentration polarization disruption, accompanied by a higher scaling potential, thus, a decreasing mass transfer over time.

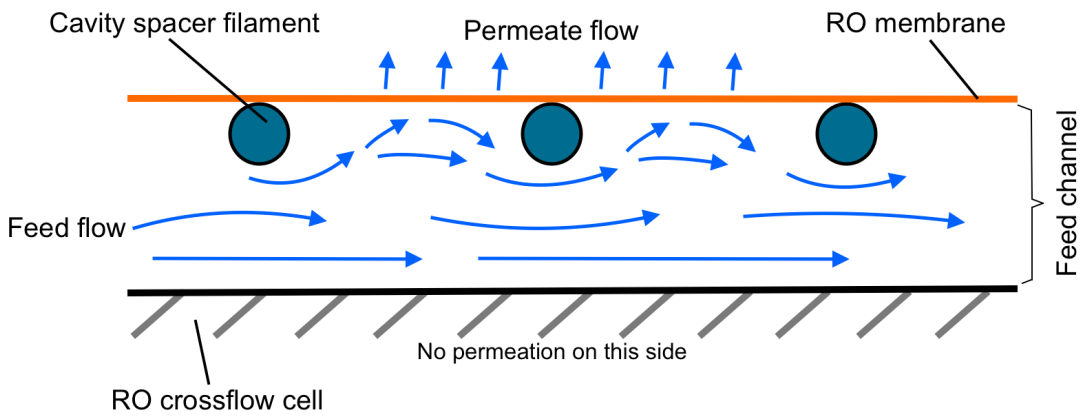


**Figure 31: Schematic cross-sectional view of one side of the cavity spacer inside the crossflow cell's feed channel.**

## 4.2 Zigzag spacer

Run 3 and 4 used the zigzag spacer. The same procedure was done as Run 1 and 2: new spacers and membranes for each run, and a 30-minute acclimatization before the start of the measurements. The operating permeate flux for Run 3 and 4 was on average 20 LMH.

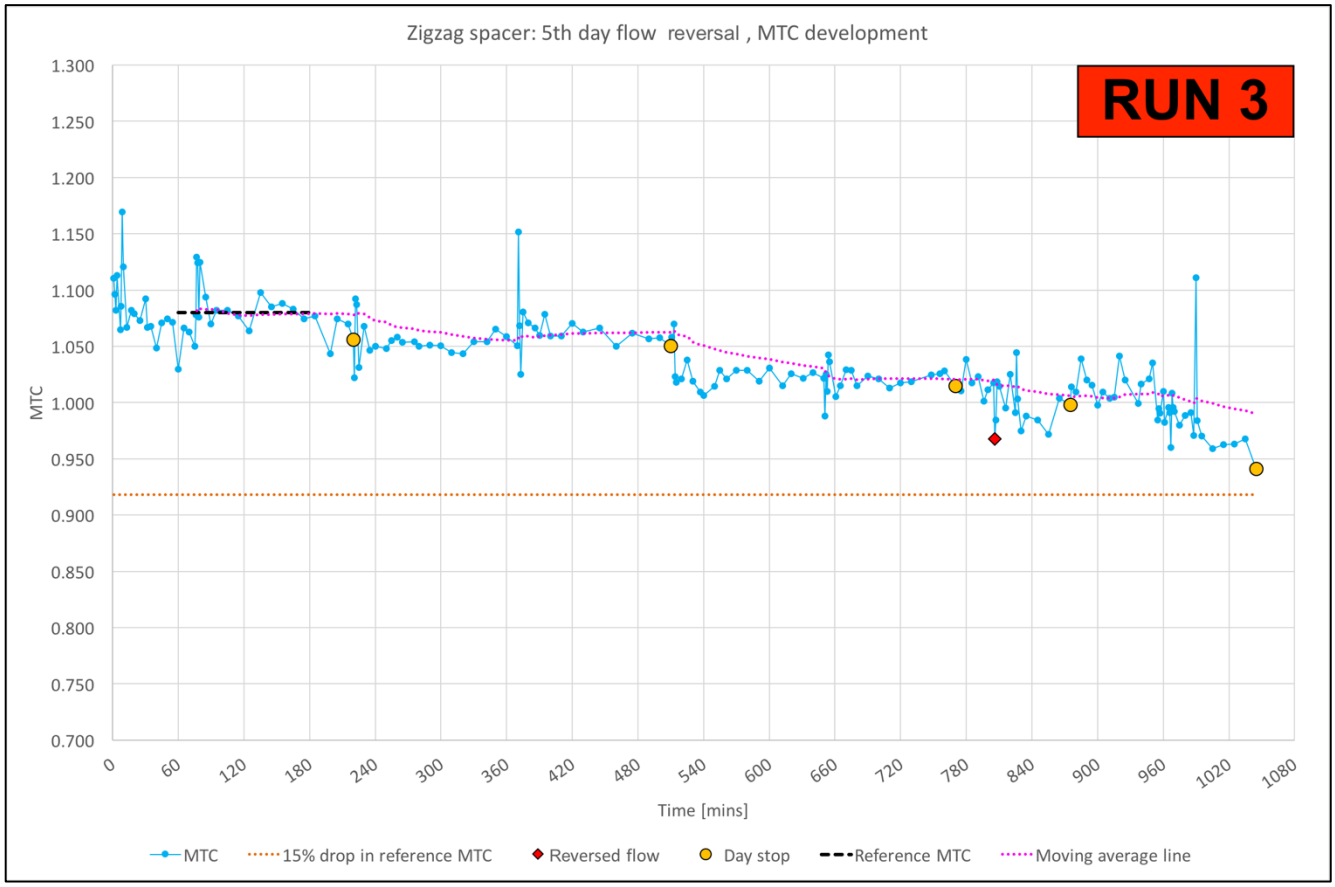


**Figure 32: MTC development for the zigzag spacer when reversing the flow direction after minute 805, which corresponds to the fifth day of Run 1. This experiment was run for approximately 1045 minutes with daily stops.**

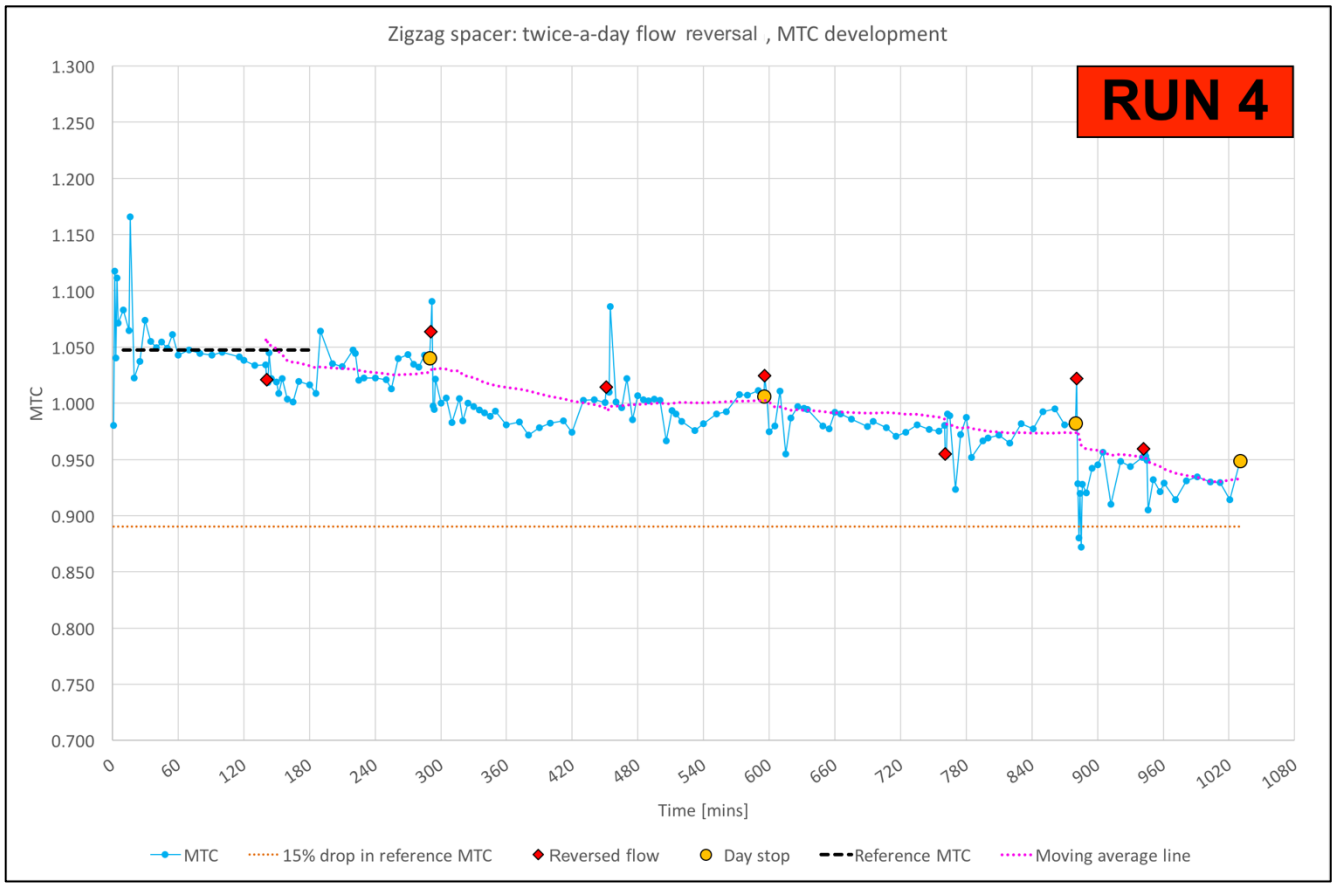


**Figure 33: MTC development for the zigzag spacer when reversing the flow direction twice a day. This experiment was run for approximately 1030 minutes with daily stops.**

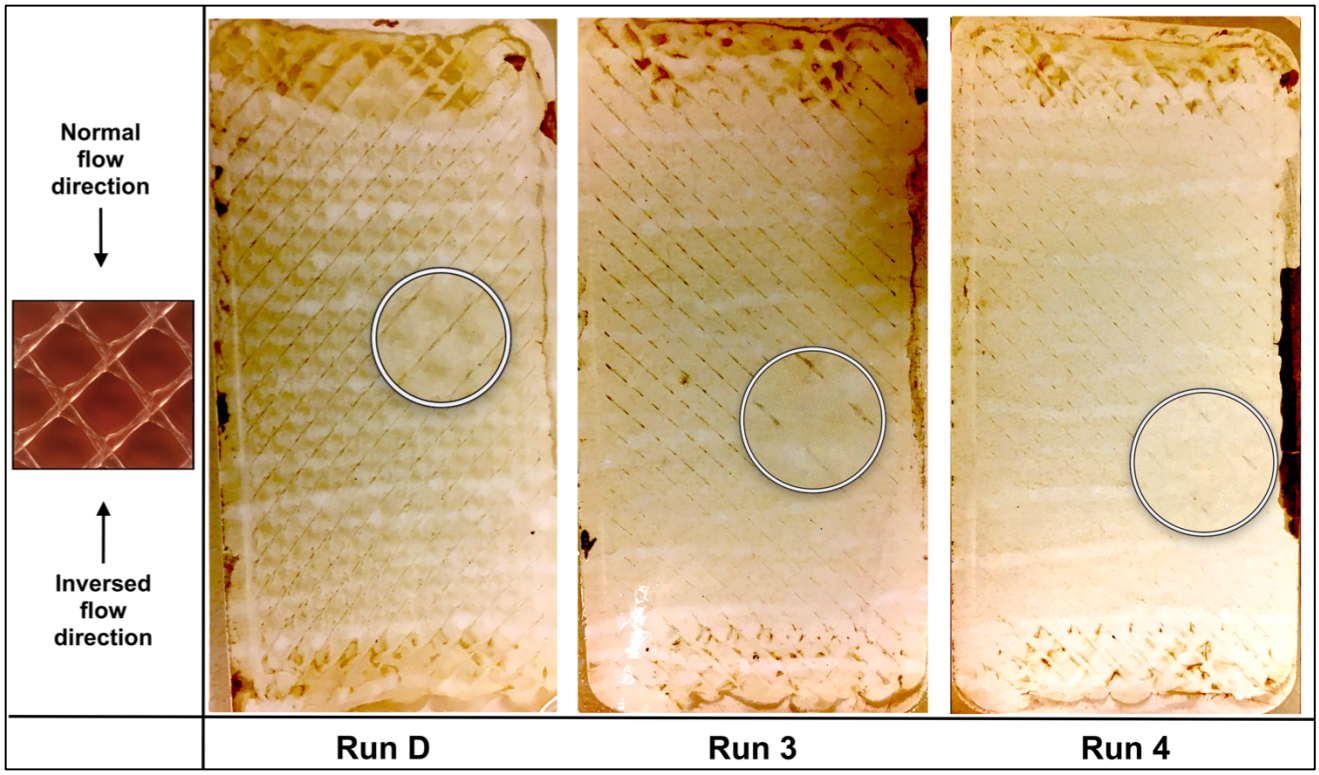


**Figure 34: Visual fouling on three different flat-sheet membranes using the zigzag spacer. For each run, a new spacer and flat-sheet membrane were used. The circles on each membrane show a zoomed-in area of visual fouling.**

From the membrane used on Run 3 and 4 shown Figure 34, the effectiveness of crossflow reversal on fouling removal cannot be properly concluded by a visual inspection. The fouling pattern on the membrane from Run 3 is almost identical to the one from Run 4.

From Figure 32 and Figure 33, it can be seen that the MTC drop follows quite the same slope development on both Run 3 and Run 4, and neither of them experience a MTC drop of 15% from the reference MTC. A crossflow reversal on minute 806 (corresponding to the same minute of the crossflow reversal of Run 1) and a twice-a-day flow reversal done on a zigzag spacer showed no significant difference in the MTC development.

The last two observations on the previous paragraph, together with the visual evaluation of fouling on Run 3 and Run 4 membranes, let us conclude that the zigzag spacer prevents organic/particulate fouling from occurring at a quicker rate compared to the cavity spacer. The MTC drop from Run 3 and 4 can then be mostly attributed to scaling.

The zigzag spacer showed a better effect on the flow mixing and the concentration polarization than the cavity spacer. A less steep negative slope of the graphed MTC, compared to the one of the cavity spacer, can be appreciated. Compared to using the cavity spacer, a higher permeate flux per unit of available driving pressure can be sustained over longer periods of time when using the zigzag spacer. It is hard to conclude from Run 3 and 4 if the frequency of crossflow reversals on this spacer has an effect on the mass transfer.

## 4.3 Pressure drop

Even though the objective of the study focuses merely on the effect that the cavity and zigzag spacer have on fouling removal, experimental results on the pressure drop caused by these spacers are also shown.

As already mentioned when justifying the average crossflow velocity in the section of "Final phase of experiments", which was 0.36 m/s, the pressure drop could only be measured for velocities above 0.35 m/s due to the low frequencies at which the pump was operating. Lower velocities could not be achieved, however, a clear difference on the pressure drop caused by each of the spacers can be seen on Figure 35.

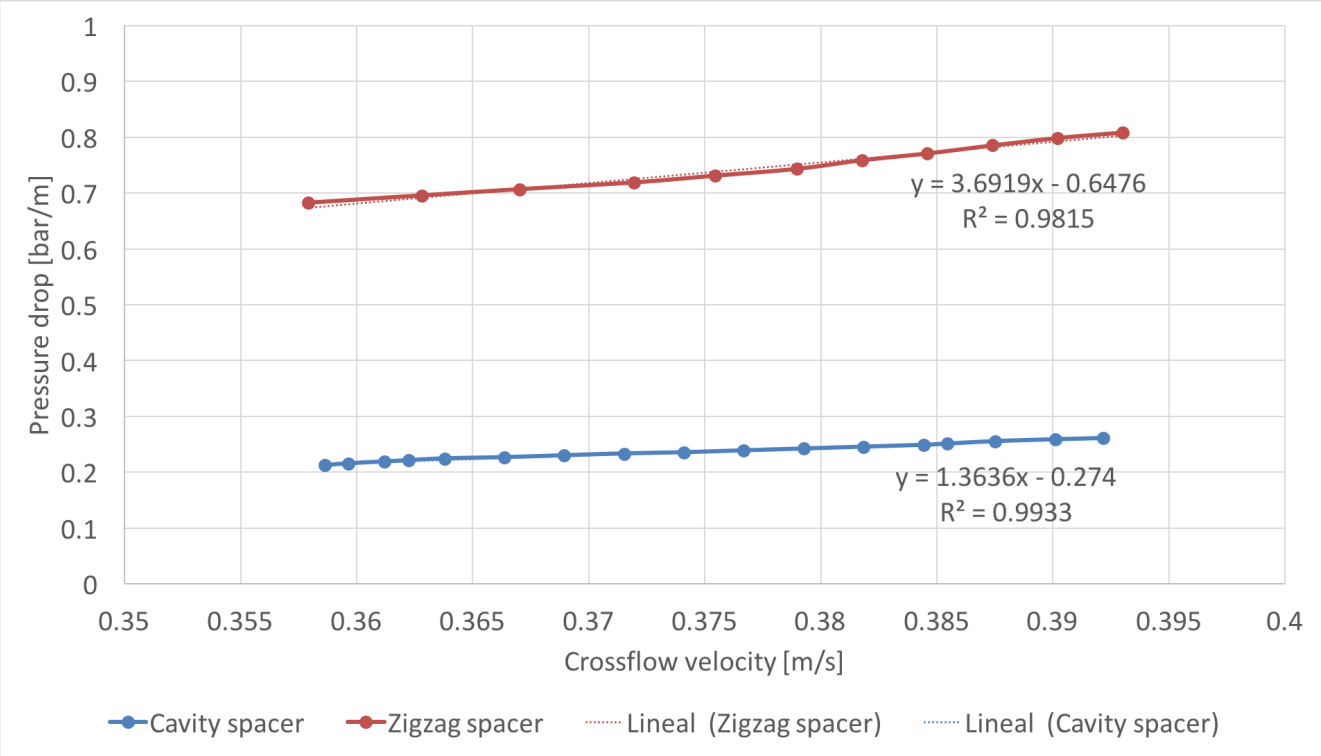


**Figure 35: Pressure drop for the cavity and zigzag spacer inside the RO crossflow cell.**

As shown on Figure 35, the cavity spacer has the lowest water resistance compared to the zigzag spacer. Assuming there are two RO elements, one with the cavity spacer and the other with the zigzag spacer, and they operate at a crossflow velocity of 0.36 m/s (same as in **the Project**), the first element with the cavity spacer will experience a 68% less pressure drop compared to the one in the element with the zigzag spacer. Both of the pressure-drop graphs for each spacer behave linearly, however, this behaviour only accounts for the range of the velocities graphed, from 0.35 to 0.40 m/s approximately. The slope of the tendency line for the zigzag spacer pressure is 2.7 times higher than the slope of the tendency line for the cavity spacer. Considering a wider range of velocities, i.e. 0.1-0.4 m/s, the graph for the zigzag spacer would behave exponentially, and the graph for the cavity spacer would remain with its linear behaviour, as shown on section 6.3.1 from the PhD thesis study of Haidari (Haidari, 2017). The graphed range of velocities on Figure 35 corresponds to a zone of high-energy consumption for the operation of an RO system. This means that if lower velocities than 0.35 m/s were used, the pressure drop for each spacer would be lower, and the difference between the pressure drop of each spacer would be less.

Having lower crossflow velocities would mean a less turbulent feed flow, with a lower shear stress, conditions which would consequently improve particulate deposition and a higher concentration polarization (Belfort et al., 1994; Koo et al., 2015). However, lower crossflow velocities also dissipate less energy, thus causing a lower pressure drop (Da Costa et al., 1994).

### 4.3.1 Pressure drop as a fraction of available driving pressure

With a crossflow velocity of 0.36 m/s, less energy is lost over an RO element with the cavity spacer than with a zigzag spacer. Moreover, as the permeate recovery rate increases in an RO system, more RO elements are required, thus, resulting in a higher total pressure drop in the system. For some of these cases, a booster pump might be required in between RO pressure vessels. However, depending on the wastewater to treat, the osmotic pressure can vary.

The magnitude of pressure losses along a spacer are relative to the feed pressure applied in the feed channel, in other words, pressure losses may become insignificant as the feed water demands a higher feed pressure. Moreover, pressure losses are lower when RO system is operated at lower crossflow velocities. By calculating the ratio between the pressure losses due to the spacer's friction and the feed pressure delivered by the pump, for the two spacers, each treating three different types of water, a better comparison can be done between the performance of each of the spacers and their applicability on each type of water in terms on energy efficiency.

The aforementioned types of water are seawater, brackish water and fresh water, which in practice demand a feed pressure of 55, 16 and 5 bars respectively (DOW, 2013). From Equation 1, the NDP can be reformulated as the following, where ΔP is the pressure drop [bar] and $\pi_f$ is the osmotic pressure [bar] in the feed:

$$NDP = P_f - \Delta P - P_p - \pi_f$$

**Equation 4**

The NDP in Equation 4 must always be equal or greater than the sum of the pressure drop, the permeate pressure and the osmotic pressure in the feed. We can then assume that the NDP is half of the feed pressure in the RO system. Considering the pressure drop that corresponds to a crossflow velocity of 0.36 m/s, as used in this study, the ratio of pressure drop to the NDP can be calculated for each type of water (seawater, brackish water and fresh water), and each type of spacer used. Figure 36 shows this ratio, assuming a pressure drop over a 6-element pressure vessel, which is a common configuration in full-scale facilities.

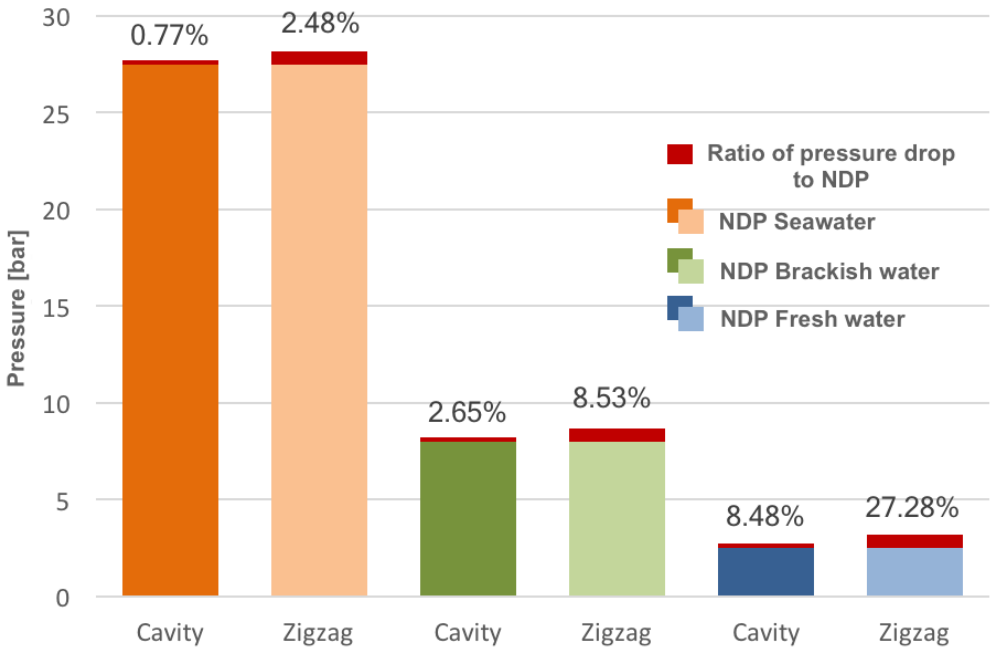


**Figure 36: Pressure drop to NDP ratios for seawater, brackish water and fresh water, for cavity and zigzag spacer at a crossflow velocity of 0.36 m/s. The ratios correspond to a situation of six RO elements.**

As seen on Figure 36, by only considering pressure drop, treating seawater with a feed spacer of either zigzag or cavity type, is basically equal. The fraction of pressure drop that corresponds to the NDP is very low on both cases. When treating brackish water, by using a zigzag spacer, the pressure drop represents almost a tenth part of the total NDP, so the cavity spacer begins to be a more attractive solution. Finally, for treating fresh water, the pressure drop reached with the zigzag spacer represents almost a third part of the NDP, making this spacer not a feasible solution, in other words, the zigzag spacer is not a recommended option when treating water that requires a very low pressure input, i.e., waters with relatively low osmotic pressure.

Nevertheless, when lower crossflow velocities are applied in RO feed channels, less pressure drop is experienced because of less turbulent flows and energy dissipation. It is important to consider that operating at lower velocities might result in a smaller difference in pressure drop between the two spacers used in this study.

### 4.3.2 Operational costs: practical case

The pressure drop results shown on Figure 35 represent an identical situation, with the same active membrane area for both of the spacers. Extrapolating the results on Figure 35 to a full-scale situation can allow an accurate comparison of the two spacers accounting pressure drop.

Furthermore, a comparison of the energy required to produce a certain volumetric flow by an RO element using each of the two spacers is done.

Manufactured RO elements for full-scale facilities have a standard size, being 8 inches the biggest diameter commercially available (DOW, 2013), however, 16-inch and 18-inch diameter elements have already been manufactured (Ng et al., 2008; Ng & Ong, 2007). Since spiral wound is the configuration for RO membranes, and feed spacers vary in thickness, the number of membrane envelopes will decrease when the spacer height increases, thus, decreasing the active membrane area in the element. So is the case of the cavity spacer.

The active membrane area for an 8-inch using the zigzag spacer (0.71 mm high) is approximately 41 $m^2$, assuming an envelope size of 1.0 x 1.0 meters in length and width. For the case of the cavity spacer (1.25 mm high), a RO element would have approximately 23 $m^2$. Assuming an RO facility with two lines, one with zigzag spacers and the other one with cavity spacers, each line with a permeate production capacity of 1000 $m^3/h$, an operation crossflow velocity of 0.36 $m/s$ (same as in **the Project**) and a permeate flux of 20 LMH, the energy consumption ($kWh/m^3$) needed to overcome the pressure drop can be calculated with Equation 5 (Da Costa et al., 1994), where $\Delta P$ is the pressure drop ($Pa/m$), $Q$ is the feed flow ($m^3/s$), $A$ is the active membrane area per RO element.

$$Energy = \Delta P \times Q \times \frac{10^{-6}}{A \times 3.6 \times Flux}$$

**Equation 5**

It is important to know that more RO elements using the cavity spacer will be needed in order to achieve the same permeate flow while operating at the same permeate flux, considering idealistic conditions in the whole system, as shown on Table 7.

**Table 7: Energy requirement per cubic meter of permeate produced, for a facility with a production capacity of 1000 m3/h**

| | ΔP [bar/m] | Crossflow vel. [m/s] | Feed flow [L/min] | Active membrane area [$m^2$] | LMH | # of elements | kWh/$m^3$ |
|---|---|---|---|---|---|---|---|
| Cavity | 0.212 | 0.36 | 0.69 | 23 | 20 | 2174 | 2.438E-07 |
| Zigzag | 0.682 | 0.36 | 0.50 | 41 | 20 | 1220 | 5.683E-07 |

From the case assumed in Table 7, it can be concluded that the zigzag spacer consumes approximately 2.3 times more energy than the cavity spacer, due to the pressure drop it

experiences when producing 1000 $m^3/h$. The cavity spacer proves to be a more energy-efficient spacer. However, the production line with the cavity spacer requires almost 1.8 times more RO elements than the line using the zigzag spacers, meaning much higher capital costs. Also, this practical case considers that every pair of membranes that constitute each RO envelope, has an equal mass transfer. This is not the case for the cavity spacer, which only has transversal filaments on one of its faces, as shown on Figure 38. This is explained in more detail on section 4.5.

## 4.4 Pollutants removal efficiencies

It is also important to know the performance of the membrane in terms of pollutant rejection. Table 8 shows the removal efficiencies for the ions in terms of electroconductivity, as well as for the COD removal, and Table 9 shows the removal efficiencies for the anions and cations, for Run 2 and 4 only.

**Table 8: RO membrane removal efficiencies for Electroconductivity and Chemical Oxygen Demand**

| | EC | COD | | | |
|---|---|---|---|---|---|
| | EC removal efficiency | RO Feed | RO Permeate | RO removal efficiency | AnMBR-RO removal efficiency |
| Run 1 | 98.05% | - | 27.2 | - | 99.75% |
| Run 2 | 97.79% | - | 103 | - | 99.06% |
| Run 3 | 96.65% | 4656 | 69.8 | 98.50% | 99.37% |
| Run 4 | 96.97% | 4875 | 86.4 | 98.23% | 99.21% |

**Table 9: RO membrane removal efficiencies for anions and cations**

| | Run 2 | | | Run 4 | | |
|---|---|---|---|---|---|---|
| | RO feed | RO permeate | Removal efficiency | RO feed | RO permeate | Removal efficiency |
| Cl- | 1257 | 32 | 97.45% | 1353 | 39 | 97.12% |
| Na+ | 4756 | 62 | 98.70% | 4221 | 85 | 97.99% |
| Mg+2 | 70 | 0 | 100.00% | 63 | 0 | 100.00% |
| K+2 | 94 | 0 | 100.00% | 74 | 31 | 58.11% |
| Ca+2 | 48 | 0 | 100.00% | 12 | 4 | 66.67% |
| SO4-2 | 48 | 0 | 100.00% | 48 | 0 | 100.00% |
| HCO3- | 7687 | 2 | 99.97% | - | 0 | 100.00% |
| Ortho-P | 0.225 | 0 | 100.00% | 0 | 0 | N/A |
| NH4+ | 0 | 0 | N/A | 26 | 22 | 15.38% |
| NO3- | 0 | 0 | N/A | 0 | 0 | N/A |

The results shown on Table 8 and Table 9, do not show good removal efficiencies. A probable explanation to this is that the active membrane area of the RO crossflow cell was no fully covered by the feed spacer, therefore allowing those uncovered areas to have a higher salt passage due to the undisrupted concentration polarization. Figure 37 shows the areas where the spacer did not have effect, and even layers of mineral scaling can be seen.

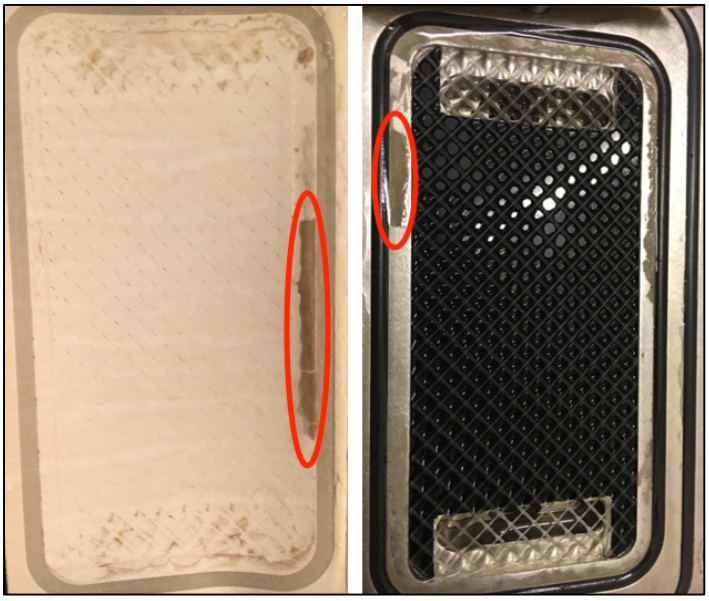

**Figure 37: Uncovered areas by the feed spacer. The red circles show the scaling that occurred on the areas where no feed spacer was acting.**

On average, membrane removal efficiencies were close to the values guaranteed by the membrane manufacturer, however, due to design problems on the crossflow cell, the results shown in this section are not fully reliable, and it can be concluded that the removal efficiencies would be even higher if the operating equipment and conditions would have been adequate.

## 4.5 General discussion

Each of the two spacers used in this study, cavity and zigzag spacer, comes with its respective advantages and disadvantages, and analysing a single result per se does not allow us to conclude on a spacer's overall performance and decide whether it is the optimal choice or not. Therefore, an integral analysis has been done and is concluded in this section.

The effect of crossflow reversal on organic/particulate fouling removal was more evident when using the cavity spacer than when using the zigzag spacer. However, this does not mean

that the zigzag spacer did not give the right conditions for fouling removal. In fact, the zigzag spacer proved to have the highest mass transfer, sustained for a longer period of time, meaning that localized turbulent flows were higher, thus having a higher effect on shear stress and continuous particle re-suspension. This previous fact is in agreement with the conclusion by Da Costa et al. (1994), which says that the hydrodynamic angle of 90° achieves the highest mass transfer, however, a higher pressure drop was achieved compared to the hydrodynamic angle of the cavity spacer (45°). This fact is also in agreement with Da Costa et al. (1994), saying that a lower hydrodynamic angle dissipates less energy, in other words, causes a lower pressure drop. These conclusions corroborate the fact that the cavity spacer, due to its hydrodynamic angle and geometry, has a (i) lower mass transfer because of the poorer effect on the flow mixing and the disruption of the concentration polarization layer, and a (ii) lower pressure drop because of the lower energy dissipation in the feed flow.

When using the cavity spacer on a spiral wound configuration, the location of the transversal filaments of the spacer do have an effect on the membrane they are in contact with, but not on the opposite membrane, meaning very probably that the RO element would have two different magnitudes of mass transfer: (i) a higher magnitude corresponding to the membrane that is in contact with the "filament side" (as shown on Figure 38), and (ii) a lower magnitude corresponding to the "cavity side".

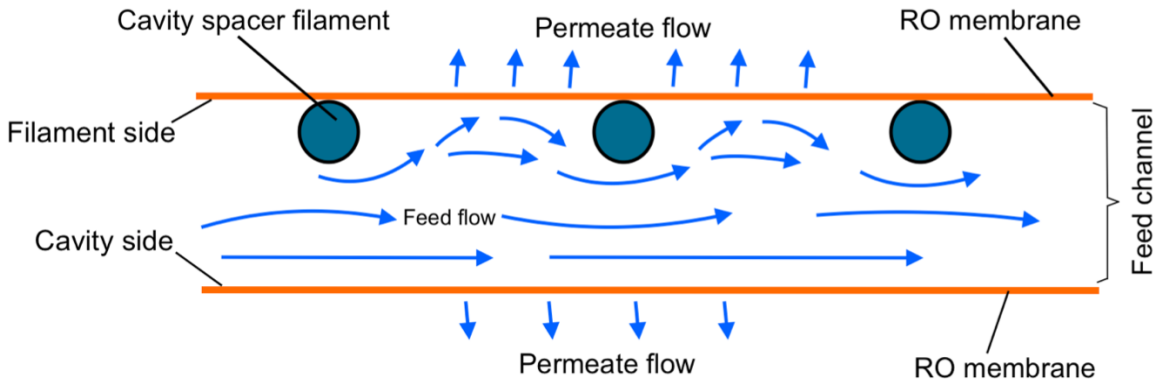


**Figure 38: Schematic cross-sectional view of one side of a cavity spacer inside a RO feed channel.**

On the other hand, one of the advantages of the cavity spacer is that particulate fouling would not be likely to occur on its cavity side, since crossflow velocities on that side would remain more constant than the filament side, and no low-velocity zones would be present, avoiding deposition of matter, and consequently biofouling on the cavity side. However, permeation drag as well as concentration polarization could cause organic/particulate fouling.

From the ratio of pressure drop to NDP calculated on section 4.3.1, and considering the conclusions on each spacer's mass transfer efficiency discussed on the second paragraph of this section, the zigzag spacer shows to be the best option for treating seawater and brackish water. However, the energy consumption analysis shows that for the crossflow velocity used in this study (0.36 m/s), the zigzag spacer is the least preferred option compared to the cavity spacer, with almost 2.3 times higher energy consumption per cubic meter, for a practical case of a facility with a permeation capacity of 1000 $m^3$/h. Nevertheless, for the same practical case, the capital costs if cavity spacers were used would be approximately 1.8 times more than when using zigzag spacers, mainly because more RO elements would be needed due to a lower active membrane area per element. Again, operational and capital costs do not consider the effect of the two different mass transfer magnitudes that the cavity spacer would cause on each of the two membranes that it is in contact with.

An increase in the pressure drop on each of the four runs from the final phase of experiments was observed from the values measured by the differential pressure meter (Endress+Hauser model Deltabar PMD75), not surpassing a 10% increase on any run. However, it cannot be concluded that this increase is merely attributed to biofouling on the spacer, since scaling and organic/particulate fouling occurring on the membrane's surface can also create resistance to the flow (Brauns et al., 2002). Moreover, no trend was found between the applied crossflow reversal frequency and the pressure drop increase on each of the runs.

The study of Haidari (2017) was a frequently referenced for the understanding of the relationship between the different crossflow velocities and the variations of these throughout time and space in the feed spacers. Nevertheless, Haidari's study (2017) did not include permeation in the crossflow cell, which is a factor directly related to permeation drag, and strongly contributes to concentration polarization, and thus, fouling.

Finally, by doing an equipment-cost analysis, new experiments with lower crossflow velocities than 0.36 m/s, as well as graphing the MTC development considering permeation on each face of the cavity spacer, a more accurate comparison of the cavity and zigzag spacer could be done. The effect of crossflow reversal on organic/particulate fouling removal would be expected to be less efficient at lower crossflow velocities.

# 5. CONCLUSIONS

- Crossflow reversal proved to be a reliable method for removing organic/particulate fouling, but it does not improve the mass transfer as chemical cleaning can.
- The zigzag spacer can help sustain a higher mass transfer for longer periods of time, due to a higher flow mixing and concentration polarization disruption, in other words, organic/particulate fouling occurs less. Nevertheless, it was not clear if more frequent crossflow reversals had a more efficient effect on organic/particulate fouling removal.
- Organic/particulate fouling was more severe when using the cavity spacer, compared to using the zigzag spacer. It can be said that the cavity spacer "induces" organic/particulate fouling, but at the same time allows it to be removed more efficiently when doing a crossflow reversal.
- The cavity spacer is approximately 2.3 times more efficient than the zigzag spacer in terms of energy consumption for crossflow velocities in the range of 0.3 and 0.4 m/s.
- The cavity spacer, due to the location of its transverse filaments, is presumed to present a "bipolar" effect on the two membranes that would be contacting each of its faces. These membranes would have differences on:
    i. Mass transfer magnitudes
    ii. Fouling types
    iii. Fouling rate

Finally, Table 10 shows a very generalized comparison of the applicability of the two spacers for different water sources, as well as their performance for different parameters.

**Table 10: Spacers comparison for different parameters**

| | Cavity | Zigzag |
|---|---|---|
| Lower fouling tendency | | X |
| Better fouling removal | X | |
| Better mass transfer | | X |
| Lower operational costs | X | |
| Lower capital costs | | X |
| Suitable for: | | |
| Seawater | | X |
| Brackish water | | X |
| Fresh water | X | |

According to the results obtained in this study from theory, practical assumptions, and lab-scale experiments, the zigzag spacer shows to be the most promising option for a wider range of water sources. The cavity spacer is a good option for treating waters with low salinity concentrations.

## 5.1 Recommendations

1. The use of cavity spacers reduces the active membrane area per RO element, consequently requiring more RO elements than when using the zigzag spacer for achieving the same permeate flow, thus, increasing capital costs. It is then proposed to opt for RO elements with bigger diameters, which have a higher active membrane area. Capital costs can then be reduced considerably.
2. If fresh water is to be treated on a full-scale RO facility, a first and isolated RO element with the cavity spacer would be an optimal selection for "inducing" organic/particulate fouling, which can be efficiently removed by a frequent crossflow reversal. Online mass transfer monitoring can be applied in order to define the frequency of the crossflow reversal according to an MTC drop. Moreover, this spacer shows the lowest ratio of pressure drop to NDP, saving energy on the first element and allowing a higher NDP for the posterior RO elements. For the second and following elements, the cavity spacer could still be used, if (i) anyhow it is assured that organics and particles were majorly removed from the system at the first RO isolated element, and if (ii) the concentration of salts in the feed has not reached a level that can be ideal for scaling formation.
3. Further research on crossflow reversal for removing particulate/organic fouling should be done in order to find the optimal frequency of the crossflow reversal.
4. A modification of the cavity spacer could be done in the future, considering the costs involved to produce the new modified spacer. The modifications are aiming at solving the face of the spacer that has no transversal filaments, which has no effect on flow mixing and concentration polarization disruption, and consequently affects the mass transfer negatively.
5. The lab-scale crossflow cell allowed excellent results, but it did not fully simulate a RO feed channel. Permeation on both faces of any spacer used should be available, as well as adjustable feed channel height to the spacer thickness.

# REFERENCES


AQUASTAT. (2016). AQUASTAT - FAO's Information System on Water and Agriculture - Water uses. *Food and Agriculture Organization of the United Nations (FAO)*. Retrieved from http://www.fao.org/nr/water/aquastat/water_use/index.stm#tables

Belfort, G., Davis, R. H., & Zydney, A. (1994). The behavior of suspensions and macromolecular solutions in crossflow microfiltration. *Journal of Membrane Science*, *96*, 1–58. Retrieved from https://ac.els-cdn.com/0376738894001197/1-s2.0-0376738894001197-main.pdf?_tid=02ab3a1c-a522-11e7-9281-00000aacb35e&acdnat=1506695295_52329c523ae7e6fcaeb825002d9d0378

Bódalo-Santoyo, A., Gómez-Carrasco, J. L., Gómez-Gómez, E., Máximo-Martín, F., & Hidalgo-Montesinos, A. M. (2003). Application of reverse osmosis to reduce pollutants present in industrial wastewater. *Desalination*, *155*(2), 101–108. https://doi.org/10.1016/S0011-9164(03)00287-X

Brauns, E., Van Hoof, E., Molenberghs, B., Dotremont, C., Doyen, W., & Leysen, R. (2002). A new method of measuring and presenting the membrane fouling potential. *Desalination*, *150*(1), 31–43. https://doi.org/10.1016/S0011-9164(02)00927-X

Bucs, S. S., Radu, A. I., Lavric, V., Vrouwenvelder, J. S., & Picioreanu, C. (2013). Effect of different commercial feed spacers on biofouling of reverse osmosis membrane systems: A numerical study. *Desalination*, *343*, 26–37. https://doi.org/10.1016/j.desal.2013.11.007

Bucs, S. S., Valladares Linares, R., van Loosdrecht, M. C. M., Kruithof, J. C., & Vrouwenvelder, J. S. (2014). Impact of organic nutrient load on biomass accumulation, feed channel pressure drop increase and permeate flux decline in membrane systems. *Water Research*, *67*(0), 227–242. https://doi.org/10.1016/j.watres.2014.09.005

Buhrmann, F., Van Der Waldt, M., Hanekom, D., & Finlayson, F. (1999). DESALINATION Treatment of industrial wastewater for reuse. *Desalination*, *124*, 263–269. https://doi.org/10.1016/S0011-9164(99)00111-3

Da Costa, A. R., Fane, A. G., & Wiley, D. E. (1994). Spacer characterization and pressure drop modelling in spacer-filled channels for ultrafiltration. *Journal of Membrane Science*, *87*(1–2), 79–98. https://doi.org/10.1016/0376-7388(93)E0076-P

DOW. (2013). Water & Process Solutions, FILMTEC ™ Reverse Osmosis Membranes: Technical Manual. *Dow Chemical Company*, 181. Retrieved from http://www.dow.com/en-us/water-and-process-solutions/products/reverse-osmosis#/accordion/F36C1D89-9385-480A-9242-575D600E6F81

DOW. (2016). DOW FILMTECTM BW30XFR-400/34 Element. Retrieved September 20, 2017, from http://msdssearch.dow.com/PublishedLiteratureDOWCOM/dh_097a/0901b8038097a0ff.pdf?filepath=liquidseps/pdfs/noreg/609-50178.pdf&fromPage=GetDoc

Fritzmann, C., Löwenberg, J., Wintgens, T., & Melin, T. (2007). State-of-the-art of reverse osmosis desalination. *Desalination*, *216*(1–3), 1–76. https://doi.org/10.1016/j.desal.2006.12.009

Gonzalez, F. D. J. (2017). *Key Performance Indicators for Reverse Osmosis: Technical Report*. Delft.

Goosen, M. F. A., Sablani, S. S., Al-Hinai, H., Al-Obeidani, S., Al-Belushi, R., & Jackson, D. (2005). Fouling of Reverse Osmosis and Ultrafiltration Membranes: A Critical Review. *Separation Science and Technology*, *39*(10), 2261–2297. https://doi.org/10.1081/SS-120039343

Haidari, A. H. (2017). *One step membrane filtration: a fundamental study (PhD thesis)*. Delft University of Technology. Retrieved from https://repository.tudelft.nl/islandora/object/uuid:4f752da9-ccb7-462a-a5f8-a75b6532fa11?collection=research

Haidari, A. H., Blankert, B., Timmer, H., Heijman, S. G. J., & van der Meer, W. G. J. (2017). PURO: A unique RO-design for brackish groundwater treatment. *Desalination*, *403*, 208–216. https://doi.org/10.1016/j.desal.2015.09.015

Haidari, A. H., Heijman, S. G. J., & van der Meer, W. G. J. (2016). Visualization of hydraulic conditions inside the feed channel of Reverse Osmosis: A practical comparison of velocity between empty and spacer-filled channel. *Water Research*, *106*, 232–241. https://doi.org/10.1016/j.watres.2016.10.012

Hydranautics. (2001). What Is Membrane Performance Normalization? Retrieved September 16, 2017, from http://www.lenntech.com/Data-sheets/Hydranautics-normaliz-L.pdf

Into, M., Jönsson, A. S., & Lengdén, G. (2004). Reuse of industrial wastewater following treatment with reverse osmosis. *Journal of Membrane Science*, *242*(1–2), 21–25. https://doi.org/10.1016/j.memsci.2003.07.027

Judd, S. (2011a). Fundamentals. In *The MBR Book* (pp. 55–207). https://doi.org/10.1016/B978-0-08-096682-3.10002-2

Judd, S. (2011b). Introduction. In *The MBR Book* (pp. 1–54). https://doi.org/10.1016/B978-0-08-096682-3.10001-0

Karthik, M., Dafale, N., Pathe, P., & Nandy, T. (2008). Biodegradability enhancement of purified terephthalic acid wastewater by coagulation-flocculation process as pretreatment. *Journal of Hazardous Materials*, *154*(1–3), 721–730. https://doi.org/10.1016/j.jhazmat.2007.10.085

Kleerebezem, R. (1999a). *Application*. *Anaerobic treatment of phthalates: microbiological and technological aspects (PhD thesis)*. Wageningen University.

Kleerebezem, R. (1999b). *Generated Waste*. *Anaerobic treatment of phthalates: microbiological and technological aspects (PhD thesis)*. Wageningen University.

Koo, C. H., Mohammad, A. W., & Suja', F. (2015). Effect of cross-flow velocity on membrane filtration performance in relation to membrane properties. *Desalination and Water Treatment*, *55*(3), 678–692. https://doi.org/10.1080/19443994.2014.953594

Lay, W. C. L., Liu, Y., & Fane, A. G. (2010). Impacts of salinity on the performance of high retention membrane bioreactors for water reclamation: A review. *Water Research*, *44*(1), 21–40. https://doi.org/10.1016/j.watres.2009.09.026

Lousada-Ferreira, M. (2011a). *Assessing membrane integrity through particle counting*. *Filterability and Sludge Concentration in Membrane Bioreactors (PhD thesis)*. Delft University of Technology.

Lousada-Ferreira, M. (2011b). *Introduction. Filterability and Sludge Concentration in Membrane Bioreactors (PhD thesis)*. Delft University of Technology.

Macarie, H., Noyola, A., & Guyot, J. P. (1992). Anaerobic treatment of a petrochemical wastewater from a terephthalic acid plant. *Water Science and Technology*, *25*(7), 223–235.

Metcalf, E., & Eddy, H. (2003). Wastewater engineering: treatment and reuse. *Tata McGraw-Hill Publishing Company Limited, 4th Edition. New Delhi, India*, 1819. https://doi.org/10.1016/0309-1708(80)90067-6

Mullin, J. W. (2001). *Crystallization*. (Butterworth Heinemann, Ed.) (4th Ed.). Oxford. https://doi.org/10.1016/B978-075064833-2/50005-X

Ng, H. Y., & Ong, S. L. (2007). A novel 400-mm RO system for water reuse and desalination. *Environmental Engineering Management*, *17*(2), 113–116. Retrieved from http://ser.cienve.org.tw/download/17-2/jeeam17-2_113-116.pdf

Ng, H. Y., Tay, K. G., Chua, S. C., & Seah, H. (2008). Novel 16-inch spiral-wound RO systems for water reclamation: a quantum leap in water reclamation technology. *Desalination*, *225*(1–3), 274–287. https://doi.org/10.1016/j.desal.2007.02.097

Radu, A. I., van Steen, M. S. H., Vrouwenvelder, J. S., van Loosdrecht, M. C. M., & Picioreanu, C. (2014). Spacer geometry and particle deposition in spiral wound membrane feed channels. *Water Research*, *64*, 160–176. https://doi.org/10.1016/j.watres.2014.06.040

Schneider, R. P., Ferreira, L. M., Binder, P., Bejarano, E. M., Góes, K. P., Slongo, E., … Rosa, G. M. Z. (2005). Dynamics of organic carbon and of bacterial populations in a conventional pretreatment train of a reverse osmosis unit experiencing severe biofouling. *Journal of Membrane Science*, *266*(1–2), 18–29. https://doi.org/10.1016/j.memsci.2005.05.006

Sterlitech. (2017). CF042 Crossflow Cell Assembly. Retrieved September 3, 2017, from https://www.sterlitech.com/cf042-crossflow-cell-cf042h.html

Subramani, A., & Hoek, E. M. V. (2008). Direct observation of initial microbial deposition onto reverse osmosis and nanofiltration membranes. *Journal of Membrane Science*, *319*(1–2), 111–125. https://doi.org/10.1016/j.memsci.2008.03.025

Thiruvenkatachari, R., Kwon, T. O., Jun, J. C., Balaji, S., Matheswaran, M., & Moon, I. S. (2007). Application of several advanced oxidation processes for the destruction of terephthalic acid (TPA). *Journal of Hazardous Materials*, *142*(1–2), 308–314. https://doi.org/10.1016/j.jhazmat.2006.08.023

UN Water. (2017). *The United Nations World Water Development Report 2017*. Retrieved from http://unesdoc.unesco.org/images/0024/002471/247153e.pdf

van Halem, D., van der Meer, W., van der Hoek, J. P., Rietveld, L., Heijman, B., & Keuten, M. (2009a). Micro- and ultrafiltration. *Drinking Water Treatment (CIE4475) TU Delft Lecture Notes*, 79–94.

van Halem, D., van der Meer, W., van der Hoek, J. P., Rietveld, L., Heijman, B., & Keuten, M. (2009b). Nanofiltration and Reverse Osmosis. *Drinking Water Treatment (CIE4475) TU Delft Lecture Notes*, 95–108.

van Lier, J. B., Mahmoud, N., & Zeeman, G. (2008). *Anaerobic Wastewater Treatment*. *Biological Wastewater Treatment : Principles, Modelling and Design*. https://doi.org/10.1021/es00154a002

Vourch, M., Balannec, B., Chaufer, B., & Dorange, G. (2008). Treatment of dairy industry wastewater by reverse osmosis for water reuse. *Desalination*, *219*(1–3), 190–202. https://doi.org/10.1016/j.desal.2007.05.013

Vrouwenvelder, J. S. (2009). Effect of feed spacer. In *Biofouling of spiral wound membrane systems* (p. 188).

Vrouwenvelder, J. S., Graf von der Schulenburg, D. A., Kruithof, J. C., Johns, M. L., & van Loosdrecht, M. C. M. (2009). Biofouling of spiral-wound nanofiltration and reverse osmosis membranes: A feed spacer problem. *Water Research*, *43*(3), 583–594. https://doi.org/10.1016/j.watres.2008.11.019

Vrouwenvelder, J. S., Van Loosdrecht, M. C. M., & Kruithof, J. C. (2011). A novel scenario for biofouling control of spiral wound membrane systems. *Water Research*, *45*(13), 3890–3898. https://doi.org/10.1016/j.watres.2011.04.046

Zimmerer, C. C., & Kottke, V. (1996). Effects of spacer geometry on pressure drop, mass transfer, mixing behavior, and residence time distribution. *Desalination*, *104*, 129–134. Retrieved from http://ac.els-cdn.com/0011916496000355/1-s2.0-0011916496000355-main.pdf?_tid=67c604c6-9b96-11e7-abd7-00000aacb35e&acdnat=1505645774_35a31c43d9bb79b78af7ee989f77acef